Effect of tidal resuspension with oyster biodeposits on nutrient and oxygen dynamics

Elka T. Porter[1],*, **Sara Blickenstaff[1,2]**, **Jeffrey C. Cornwell[3]**, **Melanie Jackson[3,4]**,
Sabrina N. Tolbert[1,2]

[1]**Yale Gordon College of Arts and Sciences, The University of Baltimore, 1420 N. Charles St., Baltimore, MD 21201, USA**
[2]**Patuxent Environmental and Aquatic Research Laboratory, Morgan State University, Saint Leonard, MD 20685, USA**
[3]**Horn Point Laboratory, University of Maryland Center for Environmental Science, Cambridge, MD 21613, USA**
[4]**NOAA Office of Legislative and Intergovernmental Affairs, Silver Spring, MD 20910, USA**

ABSTRACT: To test the effect of biodeposit resuspension on nutrient and oxygen dynamics, we performed a 30 d experiment in three 1000 l shear turbulence resuspension mesocosm (STURM) tanks (R) and three 1000 l non-resuspension (NR) tanks. All tanks contained defaunated muddy sediment and brackish estuarine water, received daily additions of oyster biodeposits, and had similar water column root mean square turbulent velocities (~1 cm s^{-1}), energy dissipation rates (~0.08 cm^2 s^{-3}), and tidal cycles (4 h mixing-on; 2 h mixing-off). While bottom shear stress was low in NR tanks, high instantaneous bottom shear produced sediment and biodeposit resuspension in R tanks during the mixing-on cycles. Resuspension and biodeposit addition resulted in complex nutrient and oxygen dynamics in the water column as well as altered seabed fluxes. Modeled biodeposit diagenesis demonstrated that added resuspended biodeposit nitrogen in R tanks was nitrified, resulting in high water column nitrate and nitrite concentrations, as well as increasing water column dissolved oxygen demand. Water column dissolved oxygen concentrations were 2.3 times lower in the R tanks than in the NR tanks, whereas deposited organic matter from biodeposits resulted in sediment dissolved oxygen uptake 3 times higher in NR versus R tanks. Sediment dissolved inorganic nitrogen uptake in NR tanks and efflux in R tanks, respectively, were mediated by microphytobenthos abundance and biodeposit deposition. Seabed and water column biogeochemical processes, as mediated by biodeposit resuspension, controlled the nutrient and oxygen balances. Biodeposit resuspension is important when evaluating oysters as support for eutrophication control.

KEY WORDS: Biodeposit · Resuspension · Nitrification · Nitrogen · Oxygen · STURM · Shear turbulence resuspension mesocosm · *Crassostrea virginica* · Benthic–pelagic coupling · Shear stress

1. INTRODUCTION

Anthropogenic disturbances and introduced diseases have contributed to the depletion of the eastern oyster *Crassostrea virginica* in Chesapeake Bay, the largest estuary on the US Atlantic coast (Newell 1988). Excessive nutrient loading and phytoplankton biomass (Kemp et al. 2005, Ator et al. 2019, Harding et al. 2019, Murphy et al. 2019) in coastal ecosystems has led to the suggestion that increasing the populations of bivalves may contribute to nutrient mitigation (Beseres Pollack et al. 2013, Bricker et al. 2014, Rose et al. 2014). Efforts to rehabilitate the oyster population through restoration (Schulte & Burke 2014) and aquaculture (Williamson et al. 2015, Ray et al. 2015) are underway. Similar approaches have

been considered in other parts of the world with similar eutrophication problems (Lindahl 2011, Holmer et al. 2015, Petersen et al. 2016, Kotta et al. 2020, Hylén et al. 2021, Ritzenhofen et al. 2021).

The euryhaline epibenthic bivalve filter feeder *C. virginica* filters large volumes of water and removes suspended microparticulate material (~2–100 μm) from the water column (Haven & Morales-Alamo 1970, Newell & Langdon 1996, Rosa et al. 2018). Filtration and nutrient assimilation into tissue with subsequent harvest (i.e. bioextraction) is considered a best management practice (BMP) to reduce nitrogen in Chesapeake Bay and elsewhere (Bricker et al. 2020). Oyster-mediated denitrification is under consideration for nutrient management (Ayvazian et al. 2021, Rose et al. 2021). However, the generation of large amounts of feces and pseudofeces as biodeposits results in the loading of particulate organic matter (POM) to the sediments (Jordan 1987) and is understudied. While some investigations suggest that bivalves reduce nutrients through conversion of bioavailable nitrogen to N_2 gas through the microbially mediated coupling of nitrification–denitrification (Newell et al. 2002, 2005, Higgins et al. 2011, Piehler & Smyth 2011, Smyth et al. 2013, Kellogg et al. 2013, 2014), others suggest that increased sediment nutrients can diminish net nitrogen removal (Lunstrum et al. 2018, Hylén et al. 2021). Thus, bivalve systems may serve as sources or sinks of nitrogen in coastal ecosystems (Smyth et al. 2018), and in some circumstances, oyster or clam aquaculture can shift sediment nitrogen processes to increased ammonium effluxes rather than denitrification (Murphy et al. 2016, Lunstrum et al. 2018).

Some of this discrepancy may exist because the impacts of the production, deposition, and fate of biodeposits on water quality and nutrient and oxygen dynamics have not been sufficiently evaluated. While it is generally assumed that oyster biodeposits remain in oyster reefs (Newell et al. 2005, Kellogg et al. 2013), some studies suggest that biodeposits can be resuspended (Colden et al. 2016, Porter et al. 2018a, 2020) and transported by currents (Lund 1957, Widdows et al. 1998, Testa et al. 2015). Hydrodynamics exert a strong influence on sediments to and from intertidal oyster reefs (Reidenbach et al. 2013). Although high biodeposition in low-flow areas can adversely affect sediments under aquaculture rafts (Cranford et al. 2007, Higgins et al. 2013), moderate rates of deposition can enhance denitrification (Newell et al. 2002, Lunstrum et al. 2018).

The highly variable rates of oyster-associated denitrification (e.g. Piehler & Smyth 2011, Higgins et al.

2013, Kellogg et al. 2013, 2014 and references therein), including directly from oyster aggregations (Caffrey et al. 2016, Arfken et al. 2017, Jackson et al. 2018), may arise either from differences in the fate of biodeposits or from the technical approach. Bottom shear stress and biodeposit resuspension have generally not been considered. No studies to date have specifically examined the effects of biodeposit resuspension in a whole-ecosystem context (but see Porter et al. 2018a, 2020a). The net biogeochemical effects of oysters on nitrogen balances have generally been determined solely within the restoration or aquaculture 'footprint' without consideration of nitrogen remineralization and denitrification from biodeposits transported away from the oyster communities.

Shear stress above the critical shear stress resuspends sediments and biodeposits, enhancing decomposition in both the water column and re-deposition sites. In experiments without resuspension, oyster-enhanced biogeochemical processes and water flow can affect the nitrogen cycle (Porter et al. 2004a). Resuspension enhances nutrient fluxes from sediments (Qin et al. 2004, Almroth et al. 2009, Corbett 2010, Porter et al. 2010, Almroth-Rosell et al. 2012, Yu et al. 2017) but also significantly affects microbial and planktonic communities and thus, ultimately, biogeochemical cycles (Wainright 1987, 1990, Porter et al. 2010, Isobe & Ohte 2014) and should be considered in whole-ecosystem experiments and models.

Our specific questions included: (1) How do resuspended biodeposits affect water column nutrient and oxygen dynamics? (2) How do resuspended biodeposits affect sediment biogeochemical nutrient and gas fluxes? To address these questions, we performed a 30 d mesocosm study focusing on the effect of biodeposit resuspension on the nitrogen cycle and oxygen dynamics, with a focus on plankton, nutrients, microphytobenthos, and biogeochemical sediment nutrient and gas fluxes.

2. MATERIALS AND METHODS

2.1. Mecocosm setup and mixing

Two sets of triplicate cylindrical tanks, the Shear TUrbulence Resuspension Mesocosm (STURM, R) tanks (Porter et al. 2018b) and standard non-resuspension (NR) tanks (termed 'C' tanks in Crawford & Sanford 2001) were set up at the Patuxent Environmental and Aquatic Research Laboratory (PEARL) at Morgan State University in St. Leonard, Maryland, in June 2018. R tanks had a single paddle (Fig. 1b,d)
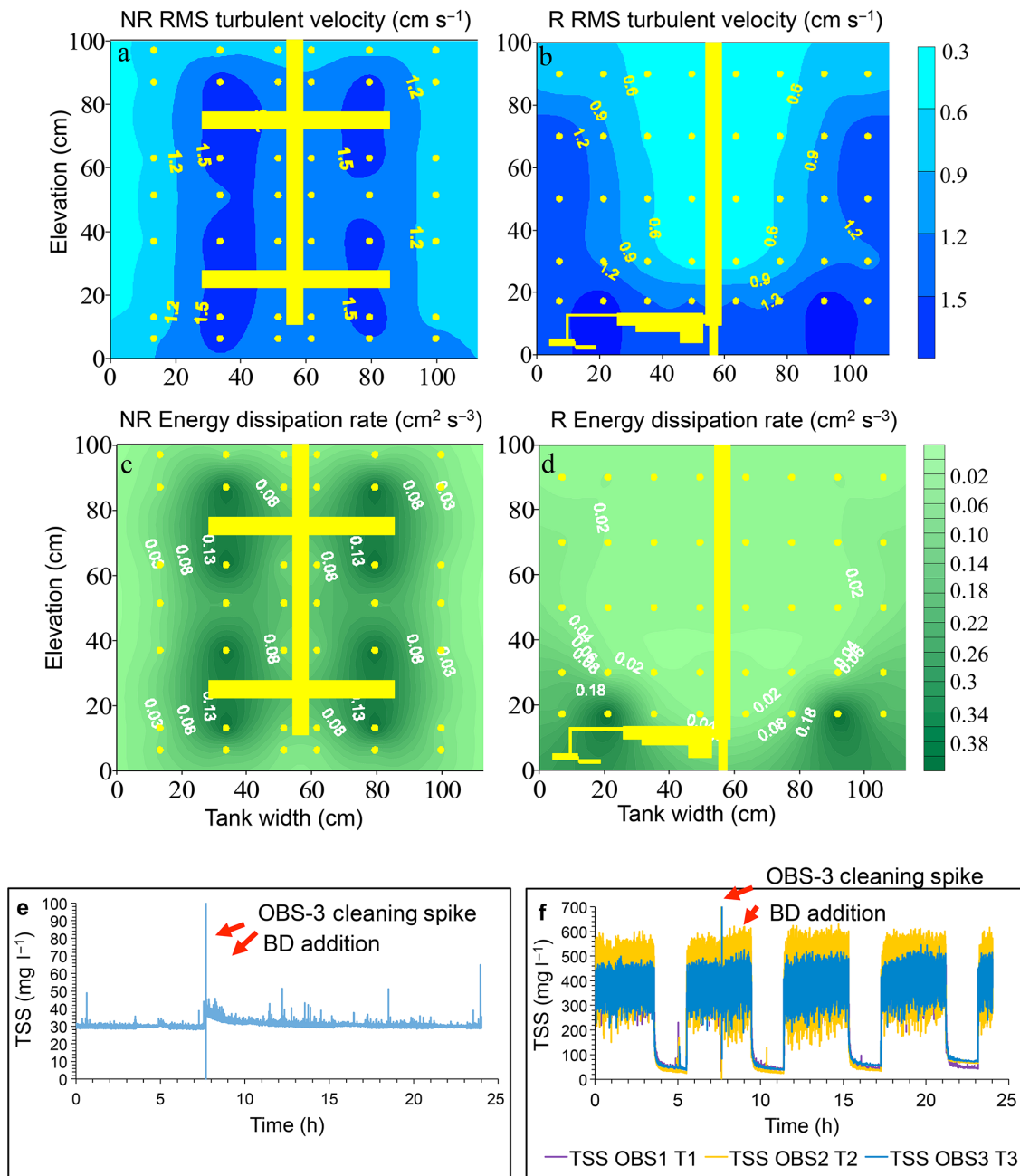
Fig. 1. Root mean square (RMS) turbulent velocity in (a) non-resuspension tanks (NR) and (b) resuspension tanks (R), with paddles in the tanks indicated in yellow. Energy dissipation rate in (c) NR tanks and (d) R tanks. Circles indicate measurement locations (a–d). Concentrations of total suspended solids (TSS) generated by tidal cycles (4 h mixing-on, 2 h mixing-off in the (e) NR tanks and (f) R tanks; n = 3 tanks each. BD: biodeposit addition, OBS-3 optical backscatter turbidity meter

to induce high bottom shear stresses which resuspended sediments and biodeposits without overmixing the water column (Porter et al. 2018b). The paddle configuration and mixing configuration in the NR tanks produced unrealistically low shear stress at the bottom and no sediment resuspension (Porter et al. 2010). The paddle speeds and forward-stop-backward-stop motion of the NR and R mixing paddles were set to produce similar tank-averaged root mean square (RMS) turbulent velocities and energy dissipation rates between the NR and R tanks. All tanks had a 1 m deep water column, a 1000 l volume, and a

1 m² sediment surface area, with a ~10 cm layer of muddy sediment at the bottom.

Benthic shear stress in the R tanks was quantified directly using hot film anemometry (Gust 1988, Porter et al. 2018b). Instantaneous bottom shear stresses were as high as 0.36–0.51 Pa in the R tanks (Porter et al. 2018b), such that sediment and biodeposit resuspension was induced during the mixing-on phases (Fig. 1f). Bottom shear stress was low (~0.001 Pa) in the NR tanks (Crawford & Sanford 2001), with no resuspension induced (Fig. 1e).

The different paddle and mixing configurations in the NR and R tanks produced water column turbulence. To calculate this turbulence, a combination of gypsum dissolution techniques (as appropriate in certain flow conditions; Porter et al. 2000) and direct flow and turbulence measurements with an acoustic Doppler velocimeter (ADV) were used at different mixing speeds at a number of representative locations in the NR and R tanks (Fig. 1a–d). An ADV was used for all turbulence measurements in the R tanks. Mixing followed cycles of 4 h on:2 h off in all systems to simulate tidal cycles throughout the 30 d experiment.

RMS turbulent velocity (cm s⁻¹) is defined in Tennekes & Lumley (1972) as:

$$q = \sqrt{\frac{1}{3}(<u^2> + <v^2> + <w^2>)} \qquad (1)$$

where $<u^2>$, $<v^2>$, and $<w^2>$ are the variances of their respective velocity components. Energy dissipation rates (cm² s⁻³) were determined following Sanford (1997). Volume-weighted RMS turbulent velocities, determined using Surfer (Golden Software), were approximately 1.08 cm s⁻¹ (Fig. 1a,b), and volume-weighted energy dissipation rates were approximately 0.0772 cm² s⁻³ during mixing-on (Fig. 1c,d); this rate is similar to the intermediate mixing treatment of Petersen et al. (1998). These turbulence levels are comparable to those used in R tanks in previous experiments comparing R vs. NR systems without biodeposits (Porter et al. 2010) and in linked mesocosms (Porter et al. 2004a,b), are lower than used in Porter et al. (2018a), and are in a realistic range (Table 1 in Sanford 1997, Porter et al. 2018b). In addition, this mixing setting kept energy dissipation rates at realistic Chesapeake Bay levels.

The mesocosms were prepared with muddy sediment, collected on 7 June 2018 from the mesohaline Patuxent estuary 38° 22' 0.9'' N, 76° 30' 0.7'' W, a tributary of Chesapeake Bay. Sediments near the sediment collection site contained 2.87 ± 0.38% carbon (min.: 2.21%; max.: 3.95%), 0.36 ± 0.04% nitrogen

(min.: 0.28%; max.: 0.47%), and 0.1 ± 0.123% phosphorus (min.: 0.010%; max.: 0.941%) (W. R. Boynton unpubl. data). Sediment was transported to PEARL (Morgan State University), where it was placed in outdoor mesocosms on 12 June 2018 after anaerobic defaunation (Porter et al. 2006). For realistic pore water gradients, sediment was equilibrated in the dark for 2 wk with a 30 cm water column of 0.5 µm filtered Patuxent estuary water (PEW) as described by Porter et al. (2006 [there Treatment HG-m], 2010, 2013, 2020). During the sediment equilibration phase in the dark, the partial water column was oxygenated via bubbling of air, and 50% of the 0.5 µm filtered PEW in the tanks was replaced daily with 0.5 µm filtered PEW for 2 wk. At the end of the sediment equilibration period, all overlying water was removed, and tanks were filled to a water column height of 1.0 m with unfiltered ambient PEW. Each day, 10% of the water in each tank was exchanged during the mixing-off phase and replaced with 0.5 µm filtered PEW to mimic tidal exchange without introducing a new plankton community.

The outside walls of all tanks were wrapped in reflective bubble wrap (Shelter Institute) to reduce overheating of the tank water during high outdoor summer temperatures (≤38°C). In addition, 2 layers of window screen mesh were placed over the superstructure ~1.5 m above the tanks to reduce insolation. Temperatures during 2 heatwaves during Days 1–4 and Days 14–16 reached up to 30.46°C in the tank water but did not exceed temperatures measured in a nearby Patuxent estuary cove (up to 31.2°C).

Light levels of ~230 µmol photons m⁻² s⁻¹ were measured at the water surface of the tanks using an LI-192 Underwater Quantum sensor (LI-COR Biosciences) attached to a model LI-250 readout. Previous experiments indicated that light levels of about 160 µmol photons m⁻² s⁻¹ are required at the water surface to prevent light limitation (Porter et al. 2004a). Therefore, any light limitation within the tanks was due to the impact of sediment and biodeposit resuspension and the resulting density of phytoplankton.

The tanks were slowly and evenly filled with pre-screened, unfiltered, 11.5 PSU salinity water containing the resident plankton community from the Patuxent estuary. Only megazooplankton >3 cm were excluded. Mixing began with programmed tidal cycles, and all tanks were synchronized. The experiment took place from 2 July to 1 August 2018 (30 d). A rainstorm added fresh water to the tanks on Day 16, reducing salinity from 11.5 to 10 PSU. On Day 20,

a major rainstorm added 10% of fresh water to each tank and reduced salinity further to 6 PSU, and by Day 21, salinity was again 9 PSU. On the evening of Day 10, software issues stopped the mixing for ~2 h during the mixing-on phase. Using a separate cleaning stick for each tank to prevent tank cross-contamination, tank walls were cleaned of periphyton every day to minimize wall growth, retaining dislodged periphyton in the tanks so wall periphyton would not affect measures of phytoplankton and zooplankton abundance (Chen et al. 1997, Chen & Kemp 2004).

During mixing-on, each of the 6 tanks received a daily addition of oyster biodeposits, starting after the first water column sampling. During the afternoon mixing-on phases, a measured volume (~2 l) of biodeposits was added to each tank; each tank received 9.71 ± 6 g dry weight of biodeposits daily. Biodeposits were generated from oysters feeding on natural plankton from the Patuxent estuary in indoor raceways with ambient PEW in continuous-flow conditions, and biodeposits were collected in trays below the oysters. Total suspended solids (TSS), particulate inorganic matter (PIM), POM, and quality (ratio of POM:PIM) of the added biodeposits were determined daily, while particulate carbon (PC), particulate nitrogen (PN), chlorophyll a (chl a), and phaeophytin concentrations were determined in biodeposits on all days except Days 2, 9, 10, and 12.

2.2. Sampling regime and variables sampled

Biological and biogeochemical measurements included water column chl a, phaeophytin, TSS, POM and PIM concentrations, phytoplankton identification and cell counts, phytoplankton pigment composition using HPLC, and water column nutrient concentrations (ammonium, nitrate plus nitrite, dissolved inorganic nitrogen [DIN], soluble reactive phosphorus [SRP], total dissolved nitrogen [TDN], total dissolved phosphorus [TDP]) with methods outlined in Table 1. Water samples (4 l) were taken at tank mid-depth during mixing-on twice a week, and for particulates, also on Days 15, 22, and 29 at the end of the mid-day mixing-off phase (Table 1). In addition, light profiles, irradiance at the bottom, geometric mean irradiance, and Secchi depth were determined during mixing-on and mixing-off (Table 1). Each morning, dissolved oxygen was measured in all tanks using a YSI Pro 20 dissolved oxygen meter (Table 1). In all R tanks, turbidity was continuously measured at 1 s intervals with optical back-scatter turbidity sensors (OBS-3; D&A Instrument) located at mid-depth (Table 1). As more OBS-3 instruments became available, starting on Day 10, turbidity was also continuously monitored in 2 NR tanks. Turbidity was calibrated with concurrently collected mid-depth TSS samples, analyzed by filtration, with weighing as described in Porter et al. (2018a).

2.3. Sediment nutrient and gas fluxes

Two sediment cores per tank were taken using a pole corer at the end of the experiment on 1 August 2018, and sediment cores were incubated in the dark and in the light at the Horn Point Laboratory, University of Maryland Center for Environmental Science, to obtain sediment gas and nutrient fluxes as affected by any microphytobenthos (Owens & Cornwell 2016). Three additional sediment cores per tank were collected and analyzed for sediment chl a (Table 1). Four additional incubations were performed on water-only as blanks to correct for water column processes. Dissolved oxygen, ammonium, nitrate plus nitrite, SRP, and dinitrogen gas concentrations were measured at 4 time points in the dark and 4 time points with illumination (Owens & Cornwell 2016) to determine nutrient and gas flux rates, corrected for the water column blanks. Solute samples were filtered (pore size: 0.45 μm) and frozen for later analysis. Samples for dissolved oxygen and dinitrogen gas were analyzed on a membrane inlet mass spectrometer (MIMS; Kana et al. 1994, 1998). Sub-cores for sediment chl a and sediment phaeophytin were collected from the flux cores and frozen at −70°C for later analysis with HPLC (Van Heukelem & Thomas 2001). Nutrients for the flux samples were analyzed colorimetrically (Jackson et al. 2018).

Nitrification efficiency (%) is an estimate of the likelihood that ammonium is transferred to nitrate plus nitrite (Kellogg et al. 2013) and was calculated from sediment biogeochemical fluxes, using $[(N_2N + NO_{2+3}) / (NO_{2+3} + NH_4 + N_2N)] \times 100$, for R and NR tanks. The denitrification efficiency (%) was an estimate that nitrogen from regeneration and from the water column was transferred to N_2 gas (Kellogg et al. 2013) and was calculated from the biogeochemical fluxes in the dark, using $[N_2N / (NH_4 + NO_{2+3} + N_2N)] \times 100$, for R and NR tanks. Nitrogen supply (sum of ammonium, nitrate plus nitrite, and dinitrogen gas fluxes; all in the light) was calculated for all flux cores, using gross O_2 production = (O_2 flux in the

Table 1. Variables measured over the 30 d ecosystem experiment in resuspension and non-resuspension tanks (n = 3 system^{-1}). Particulate and dissolved nutrients, dissolved organic carbon (DOC), chromophoric dissolved organic matter (CDOM), and chl a were analyzed by Chesapeake Biological Laboratory Analytical Services and HPLC samples by Horn Point Laboratory Analytical Services. TSS: total suspended solids; POM: particulate organic matter; PIM: particulate inorganic matter; PC: particulate carbon; PN: particulate nitrogen; PP: particulate phosphorus; DIN: dissolved organic nitrogen; TDN: total dissolved nitrogen; TDP: total dissolved phosphorus; DON: dissolved organic nitrogen; DOP: dissolved organic phosphorus; DO: dissolved oxygen; RM: repeated measures analysis, mixing-on and mixing-off; SP: split-plot analysis followed by Student-Newman-Keuls test and least square (LS) means analysis; ": same as above

Variable measured (units)	Frequency over 4 wk experiment, measured mid-depth	Analysis method used	Statistics used
Temperature (°C)	Every 10 min	Campbell T107 temperature probes (Campbell Scientific); Porter et al. (2010, 2013, 2018a, 2020)	Student-Newman-Keuls, ANOVA, LS means
Turbidity (V)	Every 1 s	OBS-3 turbidity meter, linear calibration of turbidity with TSS samples; Porter et al. (2018a)	Regression analysis[c]
Chl a and phaeo-phytin (µg l^{-1})[a]	Twice wk^{-1}; 3 times during mixing-off phase	SM10200H.3, chl a analyzed fluorometric techniques after extraction with 90% acetone, phaeophytin measured fluorometrically following acidification	RM, SP
TSS (mg l^{-1})	"	Berg & Newell (1986), Porter et al. (2018a)	"
POM (mg l^{-1})	"	Berg & Newell (1986), Porter et al. (2018a)	"
PIM (mg l^{-1})	"	Berg & Newell (1986), Porter et al. (2018a)	"
Seston quality	"	Ratio POM:PIM	"
PC, PN (mg l^{-1})	"	EPA 440.0	"
PP (mg l^{-1})	"	Aspila, EPA 365.1	"
Light profiles, irradiance) at bottom (µmol m^{-2} s^{-1})	Twice wk^{-1} mixing-on and mixing-off	LI-192 underwater quantum sensor (LI-COR Biosciences) attached to a model LI-250 readout; Porter et al. (2018a, 2020)	"
Geometric mean irradiance (µmol m^{-2} s^{-1})	"	LI-192 underwater quantum sensor (LI-COR Biosciences) attached to a model LI-250 readout; Porter et al. (2018a, 2020)	"
Secchi depth (cm)	Daily mixing-on and mixing-off	Porter et al. (2018a, 2020)	"
Phytoplankton identification and cell counts	Twice wk^{-1} mixing-on	Phytoplankton cells were counted using Utermöhl procedures (Utermöhl 1958, Marshall & Alden 1990, Lacouture 2010) as described in Porter et al. (2020)	RM
Phytoplankton pigment concentration (µg l^{-1})[a]	"	HPLC; Van Heukelem & Thomas (2001)	"
Mesozooplankton (ind. l^{-1})[a]	"	Porter et al. (2018a, 2020), Zooplankton densities (no. l^{-1}) were converted to carbon (µg l^{-1}) for each taxon following White & Roman (1992, Table 1): carbon (µg C ind.$^{-1}$) = 0.32 W	
NH$_4^+$ (µmol l^{-1})	"	Standard methods 4500-NH3 G-1997	"
NO$_3^-$ + NO$_2^-$ (µmol l^{-1})	"	ASTM D-7781/EPA 353.2	"
DIN (µmol l^{-1})	"	DIN = NO$_3^-$ + NO$_2^-$ + NH$_4^+$	"
PO$_4^{3-}$ (µmol l^{-1})	"	EPA 365.1	"
TDN (µmol l^{-1})[a]	"	Alkaline persulfate digestion, ASTM D-7781, EPA 353.2	"
TDP (µmol l^{-1})[a]	"	Alkaline persulfate digestion, EPA 365.1	"
DON (µmol l^{-1})	"	Calculated by subtracting NH$_4^+$ and NO$_3^-$ + NO$_2^-$ from TDN	"
DOP (µmol l^{-1})	"	Calculated by subtracting PO$_4^{3-}$ from TDP	"
Dissolved silicate (µmol l^{-1})	"	SM4500-SIO2 C97,11	"
DOC (mg C l^{-1})[a]	"	SM5310B	"
CDOM[a]	"	CDOM absorbance was measured over 400–700 nm, and absorbance at 440 nm for all samples was used to determine CDOM m^{-1} over time in the resuspension and non-resuspension tanks	"
DO (mg l^{-1})	Daily, in the morning	YSI Pro 20	"
Sediment chl a (µg l^{-1})[a] and sediment phaeophytin (µg l^{-1})[b]	End of experiment	HPLC, Van Heukelem & Thomas (2001)	t-test
Dark–light biogeo-chemical flux experiment	End of experiment; see Section 2.3	Owens & Cornwell (2016)	SP
Sediment %N, %C, %P, %water content	End of experiment	EPA 440.0; ASPILA, EPA 365.1	t-test

[a]Available in Table S2, Figs. S1–S4; [b]Available in Fig. S5; [c]Available in Table S1

light – O_2 flux in the dark)/6.625, and the results graphed against nitrogen demand to determine if the nitrogen supply fulfilled microphytobenthos nitrogen demand. Daily sediment dark–light fluxes were scaled for day length (Owens & Cornwell 2016), and on 1 August 2018 (the day sediment cores were collected from the mesocosms), daylight was 14.13 h and night was 9.83 h in St. Leonard, MD.

2.4. Statistical analyses

Statistical repeated-measures analysis (Crowder & Hand 1990) in SAS v.9.4 was used to assess differences (among R and NR mesocosms) for variables analyzing mixing-on phase data and for variables analyzing mixing-off data (Table 1). Samples from different dates were assessed as repeated measurements for each treatment, and p-values were calculated for testing effects of both treatment (p) and time × treatment (p2). The Greenhouse-Geisser (Greenhouse & Geisser 1959) correction was applied to p2, as necessary. In cases where the time × treatment interaction was significant, regression analysis was performed of the variable over time for both R and NR tanks, and, for specific sampling days, t-tests were performed between R and NR tanks.

A split-plot design in SAS v.8.2 was used for mixing-on–off particulate concentrations (PC, PN), on–off geometric mean irradiance, on–off irradiance at the sediment surface, as well as on–off water column chl a concentrations, phaeophytin concentrations, POM concentrations, and ratio of chl a to phaeophytin (Table 1). Moreover, a split-plot design in SAS v.8.2 was used to analyze dark–light nutrient and gas fluxes (Table 1). The Shapiro-Wilk test was used to check for normality and the Levene's test to check for homogeneous variance; data were log transformed as necessary. Post hoc tests for the split-plot design were the Student-Newman-Keuls test and least square means analyses in SAS v.8.2.

Linear regression of mesozooplankton biomass (in carbon units) and phytoplankton biomass (in carbon units estimated from direct cell counts; Strathman 1967) were used to determine the relationship between the mesozooplankton and phytoplankton communities. Linear regression was used to estimate TSS concentration from turbidity measured using OBS-3 turbidity sensors and filtered TSS samples. Regression analysis was used to compare PC, PN, particulate phosphorus (PP), and TSS concentrations. Sediment percent nitrogen, percent phosphorus, percent carbon, and percent water content, respectively,

were compared between R and NR tanks using t-tests. Statistical t-tests and regression analyses were done using the Microsoft Excel Analysis ToolPak (Microsoft); results of all analyses were considered significant at $p \leq 0.05$. Trends were defined as the $p = 0.1$–0.05 range.

2.5. Conversion of biodeposit nitrogen into labile nitrogen under resuspension

The amount of PN from biodeposits that turned into labile nitrate plus nitrite, labile ammonium, and how much was converted to dissolved organic nitrogen (DON) under resuspension over the course of the experiment in R and NR tanks was estimated, along with rates of change per day. Daily additions of biodeposits to each tank were determined (mg PN tank^{-1}), and missing biodeposit PN measurements on Days 2, 9, 10, and 12 were interpolated to determine the mg PN added to each tank via biodeposits over the 30 d experiment. Biodeposit PN (mg tank^{-1}) was converted to µmol biodeposit nitrogen per tank for each day of the experiment and used as a model input. Biodeposit nitrogen diagenesis was then modeled, based on daily added biodeposit nitrogen, using rates and proportions from Testa et al. (2015) and Brady et al. (2013) to assess how much new nitrogen from biodeposits was available and how it might be distributed in the ecosystem. To determine what nutrient species the biodeposit nitrogen would convert to, we determined cumulative nitrate plus nitrite (ΣNO_x), cumulative ammonium (ΣNH_4), and cumulative DON (ΣDON) in the water column over the 30 d experiment in R and NR tanks (n = 3 for each system; means ± SD) using Eqs. (2) & (3):

$$\text{Net } NO_x = \\ \mu\text{mol}\frac{N}{\text{tank}}\text{day2} - \mu\text{mol}\frac{N}{\text{tank}}\text{day1} + \left(0.1 \cdot \mu\text{mol}\frac{N}{\text{tank}}\text{day1}\right) \\ - \mu\text{mol N added with daily water exchange} \quad (2)$$

$$\text{Cumulative } NO_x = \\ \text{Cumulative } NO_x \text{ the day before} \\ + \text{Net } NO_x \text{ the day of} \quad (3)$$

All tanks received daily additions of oyster biodeposits, and we compared the cumulative nitrogen amounts over the experiment with the modeled amount of nitrogen available from added biodeposits. Phytoplankton biomass, zooplankton biomass, and their nitrogen contents, respectively, were not significantly different between treatments, thus affected the nitrogen budget similarly in R and NR tanks.

Table 2. Means (±SD) of variables analyzed over the experiment for resuspension (R) and non-resuspension (NR) tanks, all with daily biodeposit additions (n = 3 treatment^{-1}). All systems contained muddy sediments. Repeated measures analyses for mixing-on and mixing-off data, respectively, were performed using SAS v.9.4. Samples from different dates were assessed as repeated measurements for each treatment, and p-values were calculated for testing effects of both treatment (p) and time × treatment (p2). The Greenhouse-Geisser (Greenhouse & Geisser 1959) correction was applied to p2 as necessary. Sediment results are from the end of the experiment and were analyzed using t-tests. Results were considered significant at p ≤ 0.05 (in **bold**). Included in the analysis were all days including Day 1, on which no biodeposits had yet been added to any system. See Table 1 for definitions

Variable mixing-on / mixing-off analyzed	R Mean ± SD	NR Mean ± SD	Days	p	p2
(a) Seston (filtered samples)					
TSS, mixing-on (mg l^{-1})	325.5 ± 154.5	22.4 ± 1.5	1−29	**0.0018**	0.1998
PIM, mixing-on (mg l^{-1})	261.2 ± 128.7	10.0 ± 0.9	1−29	**0.0019**	0.1985
POM, mixing-on (mg l^{-1})	64.32 ± 26.0	12.43 ± 2.0	1−29	**0.0015**	0.2056
Ratio POM:PIM mixing-on	0.28 ± 0.06	1.21 ± 0.21	1−29	**<0.0001**	0.3024
Percent POM mixing-on	21.49 ± 3.77	53.03 ± 4.52	1−29	**<0.0001**	0.3344
TSS, mixing-off (mg l^{-1})	27.14 ± 3.26	26.67 ± 2.8	3×	0.8652	**0.0136**
PIM, mixing-off (mg l^{-1})	16.68 ± 2.43	13.69 ± 1.75	3×	0.1579	**0.0144**
POM, mixing-off (mg l^{-1})	10.45 ± 1.1	13.59 ± 1.83	3×	0.0565	**0.0167**
Ratio POM:PIM, mixing-off	0.65 ± 0.04	0.93 ± 0.05	3×	**0.0015**	0.5331
Percent POM, mixing-off	38.93 ± 1.34	48.65 ± 0.86	3×	**0.0008**	**0.0188**
(b) Particulate nutrients					
PP, mixing-on (mg l^{-1})	0.73 ± 0.37	0.07 ± 0.01	1−29	**0.0024**	0.1564
PC, mixing-on (mg l^{-1})	19.58 ± 9.79	2.14 ± 0.31	1−29	**0.0020**	0.1812
PN, mixing-on (mg l^{-1})	2.88 ± 1.44	0.40 ± 0.06	1−29	**0.0023**	0.1828
Ratio PC:PN mixing-on	6.78 ± 0.08	5.4 ± 0.04	1−29	**<0.0001**	0.3530
PP, mixing-off (mg l^{-1})	0.06 ± 0.01	0.07 ± 0.01	3×	0.2844	**0.0067**
PC, mixing-off (mg l^{-1})	1.84 ± 0.33	3.25 ± 1.56	3×	0.1985	0.1579
PN, mixing-off (mg l^{-1})	0.30 ± 0.06	0.42 ± 0.01	3×	**0.0233**	**0.0489**
Ratio PC:PN, mixing-off	6.24 ± 0.07	5.50 ± 0.07	3×	**0.0005**	**0.0046**
(c) Phytoplankton ID					
Total phytoplankton carbon, mixing-on (µg C l^{-1})	1590 ± 1055	1142 ± 1488	1−29	0.0637	**0.0020**
Phytoplankton nitrogen, mixing-on (µg N l^{-1})	240 ± 159	172 ± 225	1−29	0.0637	**0.0020**
Diatoms, mixing-on (µg l^{-1})	1310 ± 984	817 ± 1448	1−29	0.0802	**0.0013**
Phytoflagellates, mixing-on (µg l^{-1})	233 ± 137	231 ± 116	1−29	0.9629	0.2671
Dinoflagellates, mixing-on (µg l^{-1})	26.5 ± 51.3	87.5 ± 127.5	1−29	0.1964	0.1055
(d) Dissolved oxygen, dissolved nutrients					
Dissolved oxygen, mixing-on (mg l^{-1})	2.49 ± 0.29	5.72 ± 0.35	0−30	**<0.0001**	**0.0124**
NO$_3^-$ + NO$_2^-$, mixing-on (µmol l^{-1})	19.66 ± 4.42	7.09 ± 4.66	1−29	**0.0004**	0.0920
DIN, mixing-on (µmol l^{-1})	21.13 ± 4	12.27 ± 7	1−29	**0.0026**	0.1225
DON, mixing-on (µmol l^{-1})	18.24 ± 2.65	24.37 ± 1.53	1−29	**0.0013**	0.2989
DOP, mixing-on (µmol l^{-1})	0.29 ± 0.1	0.53 ± 0.1	1−29	**0.0034**	0.2504
NH$_4^+$, mixing-on (µmol l^{-1})	1.47 ± 0.82	5.18 ± 3.7	1−29	**<0.0001**	**0.0440**
Soluble reactive phosphorus (SRP) mixing-on (µmol l^{-1})	1.46 ± 0.47	1.21 ± 0.63	1−29	**0.0373**	**0.0019**
Dissolved silicate, mixing-on (µmol l^{-1})	108.76 ± 21.4	106.21 ± 21.76	1−29	0.5208	**0.0150**
TDP, mixing-on (µmol l^{-1})	1.75 ± 0.53	1.75 ± 0.69	1−29	0.4937	**0.0396**
TDN, mixing-on (µmol l^{-1})	39.36 ± 4.4	36.64 ± 7.97	1−29	0.2584	0.2058
Ratio DIN:SRP mixing-on	7.36 ± 2.96	6.59 ± 6.51	1−29	0.3814	0.0645
Ratio dissolved silicate:SRP, mixing-on	78.43 ± 11.04	147.78 ± 121.31	1−29	0.0784	0.4203
(e) Total nutrients					
Total nitrogen (TN), mixing-on (µmol l^{-1})	199.81 ± 79.51	53.25 ± 14.92	1−29	**0.0029**	0.1957
Total phosphorus (TP), mixing-on (µmol l^{-1})	19.91 ± 8.92	3.5 ± 0.53	1−29	**0.0024**	0.1681
Ratio TN:TP mixing-on	10.58 ± 0.92	15.11 ± 2.98	1−29	0.0876	**0.0081**
(f) Light penetration					
Irradiance at sediment surface, mixing-on (µmol photons m^{-2} s^{-1})	0.1 ± 0.24	41.79 ± 25.56	2−27	**0.0012**	0.2718
Geometric mean irradiance, mixing-on (µmol photons m^{-2} s^{-1})	2.85 ± 3.76	121.39 ± 61.9	2−27	**0.0009**	0.1886
Secchi depth, mixing-on (cm)	29.94 ± 8.41	68.35 ± 22.79	0−30	**<0.0001**	**<0.0001**

Table 2 (continued)

Variable mixing-on / mixing-off analyzed	R Mean ± SD	NR Mean ± SD	Days	p	p2
Irradiance at sediment surface, mixing-off (μmol photons m^{-2} s^{-1})	36.28 ± 22.78	35.62 ± 19.20	2–27	0.8476	0.2132
Geometric mean irradiance, mixing-off (μmol photons m^{-2} s^{-1})	106.81 ± 63.03	126.71 ± 58.6	2–27	0.0936	0.0819
Secchi depth, mixing-off (cm)	59.29 ± 10.96	65.75 ± 22.85	0–30	**0.0003**	**0.0012**
(g) Sediment (*t*-tests)					
Percent carbon in top 0.5 cm	3.72 ± 0.49	3.66 ± 0.49	Day 30	0.2920	
Percent nitrogen in top 0.5 cm	0.48 ± 0.08	0.47 ± 0.08	Day 30	0.2355	
Percent phosphorus in top 0.5 cm	0.1 ± 0.03	0.09 ± 0.07	Day 30	0.1376	
Percent water content in top 0.5 cm	83.23 ± 4.35	81.86 ± 3.15	Day 30	0.5863	
Sediment chl *a* in top cm (mg m^{-2})	105.9 ± 58.9	89 ± 19.4	Day 30	0.6831	
Sediment phaeophytin in top cm (mg m^{-2})	140.8 ± 143.7	47 ± 17.8	Day 30	0.3787	
Sediment chlorophyllide in top cm (mg m^{-2})	17.4 ± 7.5	71 ± 17.8	Day 30	**0.0172**	

(h) Biodeposit additions
PC (mg C tank^{-1}) daily added 825.66 ± 469.18 mg d^{-1}
PN (mg N tank^{-1}) daily added 126.55 ± 72.19 mg d^{-1}
PP (mg P tank^{-1}) daily added 29.29 ± 15.27 mg d^{-1}
TSS (g TSS tank^{-1}) daily added 9.71g ± 6 g d^{-1}
POM (g POM tank^{-1}) daily added 2.7 ± 1.4 g d^{-1}
Chl *a* (mg chl *a* tank^{-1}) daily added 2.45 mg ± 1.92 mg d^{-1}
Phaeophytin (mg Phaeophytin tank^{-1}) daily added 7.15 ± 3.30 mg d^{-1}

3. RESULTS

See Tables 2 & 3, Figs. 1–9 for results of the bio-deposits added to each of the 6 tanks, seston and particulate nutrients, phytoplankton, dissolved oxygen, dissolved nutrients and total nutrients, light penetration, microphytobenthos, sediment nutrient and gas fluxes, and the conversion of biodeposit nitrogen into labile nitrogen under resuspension. In addition, we provide results for phytoplankton pigments and meso-zooplankton, other ancillary results, in Tables S1–S2 and Figs. S1–S5 in the Supplement at www.int-res.com/articles/suppl/m686p037_supp.pdf.

Water temperatures ranged from 22.61–30.46°C in the experiment (R tanks: 26.30 ± 0.04°C; NR tanks: 26.34 ± 0.18°C), and temperatures in the 6 tanks tracked each other closely (p = 0.7621). Water temperatures were ~2.5°C warmer over the first part of the experiment from Days 0–5 and ~2°C warmer over Days 10–17, during which the experiment experienced 2 heatwaves.

3.1. Biodeposits added

On average, 9.7 ± 6 g dry weight TSS, 826 ± 570 mg PC, 127 ± 72 mg PN, and 29.3 ± 15.3 mg PP in the biodeposits were added to each tank daily, i.e. per

m^{-2} (Table 2h), with a POM:PIM ratio of 0.6 ± 0.3. Newell et al. (2002) defined low, medium, and high biodeposit additions as 0.25, 2.5, and 5 g C m^{-2} d^{-1}, respectively; our biodeposit additions were in the medium range. Small amounts of chl *a* (2.45 ± 1.92 mg) and phaeophytin (7.15 ± 3.3 mg) were found in biodeposits and added to the tanks with the biode-posits daily. Biodeposit nitrogen diagenesis, modeled using the measured daily added biodeposit nitrogen from this experiment as inputs in the model and using rates and proportions from Testa et al. (2015) and Brady et al. (2013), resulted in 58 644 μmol nitrogen from biodeposits added to the tanks over the 30 d experiment.

3.2. Seston and particulate nutrients

TSS concentrations, as determined from OBS-3 turbidity measurements calibrated with TSS samples (Table S1), were significantly higher in R tanks with added oyster biodeposits (325.5 ± 154.5 mg l^{-1}) than in the NR tanks with added biodeposits (22.4 ± 1.5 mg l^{-1}) (p = 0.0018; Fig. 2a,b, Table 2a). TSS in R tanks came from resuspended bottom sediment plus resuspended oyster biodeposits (Fig. 1f, Table 2h). TSS and biodeposits in the R tanks were resuspended during mixing-on of the tidal cycle due to
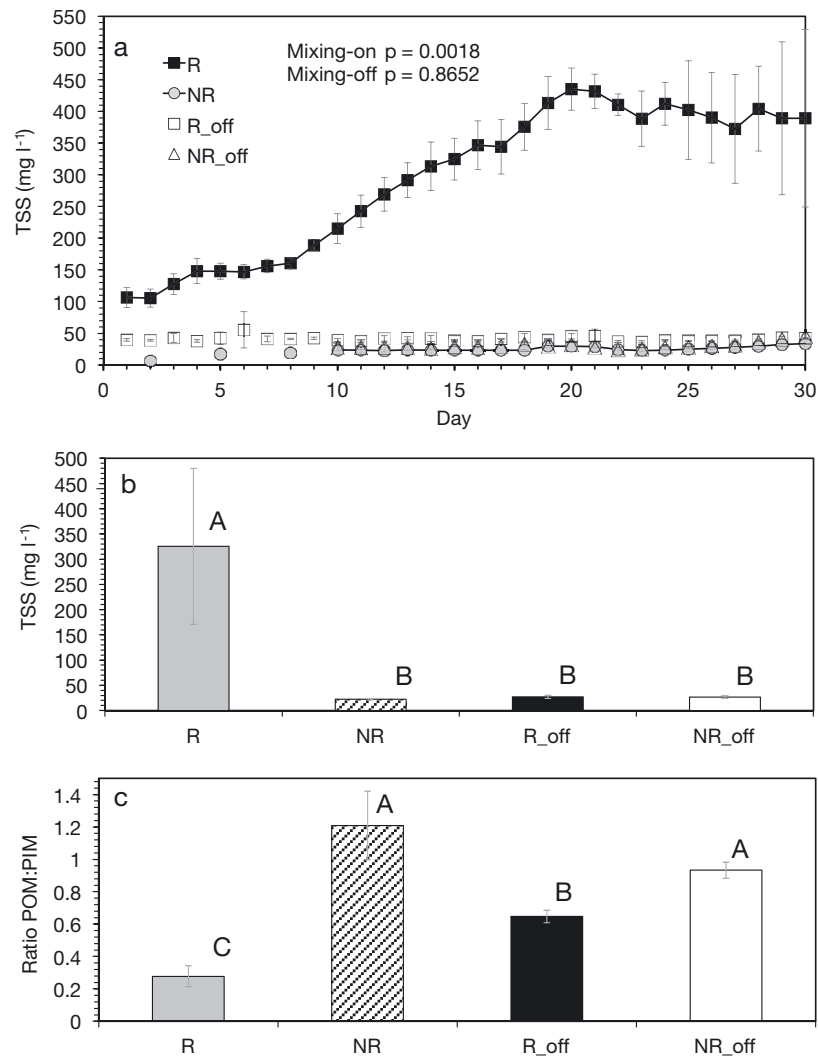
Fig. 2. (a) Mean (±SD) total suspended solid (TSS) concentrations over time in resuspension tanks (R, n = 3) and non-resuspension tanks (NR, n = 2) during the mixing-on and mixing-off phases as measured using OBS-3 sensors, calibrated with TSS samples. (b) Mean (±SD) TSS concentrations from filtered samples in (a) as analyzed using a split-plot analysis (R: n = 3; NR: n = 3). Particulate carbon, particulate nitrogen, particulate phosphorus, and particulate organic matter (not shown here) all showed exactly the same patterns and statistical results as TSS in (b). (c) Mean (±SD) seston quality, i.e. the ratio of particulate organic matter (POM) to particulate inorganic matter (PIM) in R (n = 3) tanks and NR (n = 3) tanks during the mixing-on and mixing-off phases. Samples on Day 1 were taken before biodeposits had been added to the tanks, which thereafter received oyster biodeposit additions daily over the 30 d experiment. Different letters in (b) and (c) indicate statistical differences (p ≤ 0.05). All tanks received a daily addition of oyster biodeposits

high bottom shear stress, whereas TSS and biodeposits were deposited in NR tanks with low bottom shear stress. Throughout the experiment, TSS concentrations increased from ~100 mg l^{-1} during Days 0–10 of the experiment in the R tanks to ~400 mg l^{-1} in the second half of the experiment (Days 20–30) (Fig. 2a) as 270 mg l^{-1} of biodeposit TSS were added and resuspended over the 30 d experiment (Table 2h). TSS concentrations stayed at ~25 mg l^{-1} throughout the experiment in the NR tanks (Fig. 2a,b) and did

not increase over time as added biodeposits settled out under low bottom shear stress. TSS concentrations during R tank mixing-off were not significantly different from TSS concentrations in NR tanks during mixing-on and mixing-off (Fig. 2b).

Water column POM concentrations were significantly higher in R tanks (64.32 ± 26.0 mg l^{-1}) during mixing-on than in NR tanks (12.43 ± 2.0 mg l^{-1}) (p = 0.0015; Fig. S1d,h, Table 2a). POM concentrations (Fig. S1h) followed TSS results and statistics in

Table 3. Linear relationship of total suspended solids (TSS) and particulate carbon (PC), particulate nitrogen (PN), and particulate phosphorus (PP) (all in mg l^{-1}), and linear relationship between PN and PC

Regression	R^2	n	p
PC = 0.0583 × TSS	0.98	80	<0.0001
PN = 0.0086 × TSS	0.97	77	<0.0001
PP = 0.0022 × TSS	0.98	81	<0.0001
PN = 0.1479 × PC	1.0	40	<0.0001

Fig. 2b exactly. The POM:PIM ratio, an indicator of seston quality, was significantly higher in NR tanks than R tanks during mixing-on and mixing-off (Fig. 2c, Table 2a). Seston quality increased in R tanks during mixing-off compared to mixing-on (Fig. 2c) when particles settled out.

Water column PC, PN, and PP concentrations were linearly related to TSS concentrations (p < 0.0001; Table 3), and PC, PN, and PP concentrations were significantly enhanced in R tanks compared to NR tanks (Table 2b). PC, PN, and PP concentrations followed TSS results and statistics in Fig. 2b exactly. Much of the PN, PC, and PP settled out during mixing-off phases in the R tanks and did not resuspend throughout the experiment in the NR tanks. The C:N ratio was significantly higher in R tanks than in NR tanks during mixing-on (p < 0.0001) and mixing-off (p = 0.0005; Table 2b).

3.3. Phytoplankton

In R tanks, phytoplankton biomass was dominated by diatoms throughout the experiment (Fig. 3e), while diatoms only became dominant in NR tanks during Days 25 and 29 (Fig. 3f). Total phytoplankton carbon-, diatom-, phytoflagellate-, and dinoflagellate-biomass, as determined by phytoplankton identification, did not significantly differ between R and NR tanks (Table 2c); however, there was a significant time × treatment interaction for phytoplankton carbon and diatoms. As diatom biomass increased significantly over time in the R (p = 0.0365) and NR tanks (p = 0.0445), phytoplankton carbon significantly increased over time in the R (p = 0.0173) and NR tanks (p = 0.0447). Phytoplankton nitrogen concentrations were similar between the R and NR tanks (p = 0.0637; Table 2c) and significantly increased over time in the R (p = 0.0173) and NR tanks (p = 0.0447). Phytoplankton pigment results and results on mesozooplankton abundance can be found in Text S1 & S2 in the Supplement.

3.4. Dissolved oxygen, dissolved nutrients, and total nutrients

Dissolved oxygen concentrations were about twice as high in NR tanks (5.72 ± 0.35 mg^{-1}) than in R tanks (2.49 ± 0.29 mg^{-1}) throughout the experiment (p < 0001; Fig. 4). The R tanks dipped into hypoxia (i.e. dissolved oxygen concentrations sufficiently low to negatively affect biological and ecological processes but often functionally defined as <2 mg l^{-1}; Vaquer-Sunyer & Duarte 2008) on Days 15–17, 22–26, and 30, whereas NR tanks remained well oxygenated (Fig. 4). Dissolved oxygen had a significant time × treatment interaction (Table 2d), and R tanks experienced a significant decrease in dissolved oxygen over time (p = 0.0012) whereas NR tanks did not (p = 0.6571).

Nitrate plus nitrite concentrations were about 3 times higher throughout the experiment in R tanks (19.66 ± 4.42 µmol l^{-1}) than in NR tanks (7.09 ± 4.66 µmol l^{-1}) (p = 0.0004; Fig. 5c, Table 2d). DIN concentrations were significantly higher in R than NR tanks, both of which received biodeposits, and were only briefly limiting (i.e. <2 µmol l^{-1}; Fisher et al. 1992) from Days 4–6 in NR tanks (p = 0.0026; Fig. 5d, Table 2d). Dissolved organic phosphorus (DOP) concentrations were significantly higher in NR tanks (0.53 ± 0.1 µmol l^{-1}) than R tanks (0.29 ± 0.1 µmol l^{-1}) (p = 0.0034; Fig. 5g, Table 2d). DON concentrations were significantly higher in NR tanks (24.37 ± 1.53 µmol l^{-1}) than R tanks (18.24 ± 2.65 µmol l^{-1}) (p = 0.0013; Fig. 5f, Table 2d). Moreover, dissolved organic carbon (DOC) concentrations were significantly higher in NR tanks (280.76 ± 28.82 µmol l^{-1}) than in R tanks (244.07 ± 39.05 µmol l^{-1}) (p = 0.0268; Fig. S3f, Table S2d).

Total nitrogen (TN: NH_4^+ + NO_2^- + NO_3^- + DON + PN) concentrations increased from about 74 to about 270 µmol l^{-1} in R tanks, increased from 43 µmol l^{-1} in NR tanks over the course of the experiment to 81 µmol l^{-1}, and were significantly higher in R tanks (p = 0.0029; Fig. S3d, Table 2e). Total phosphorus (TP: SRP + DOP + PP) concentrations increased from 6–29 µmol l^{-1} in R tanks (Fig. S3c), stayed around 3.5 µmol l^{-1} in NR tanks over the course of the experiment, and were significantly higher in R tanks than in NR tanks (p = 0.0024; Fig. S3c, Table 2e). Nitrate plus nitrite, DIN, DOP, DON, DOC, TN, and TP did not have a significant time × treatment interaction (Table 2d).

Ammonium, SRP, and chromophoric dissolved organic matter (CDOM) absorbance were also significantly different between R and NR tanks; however,
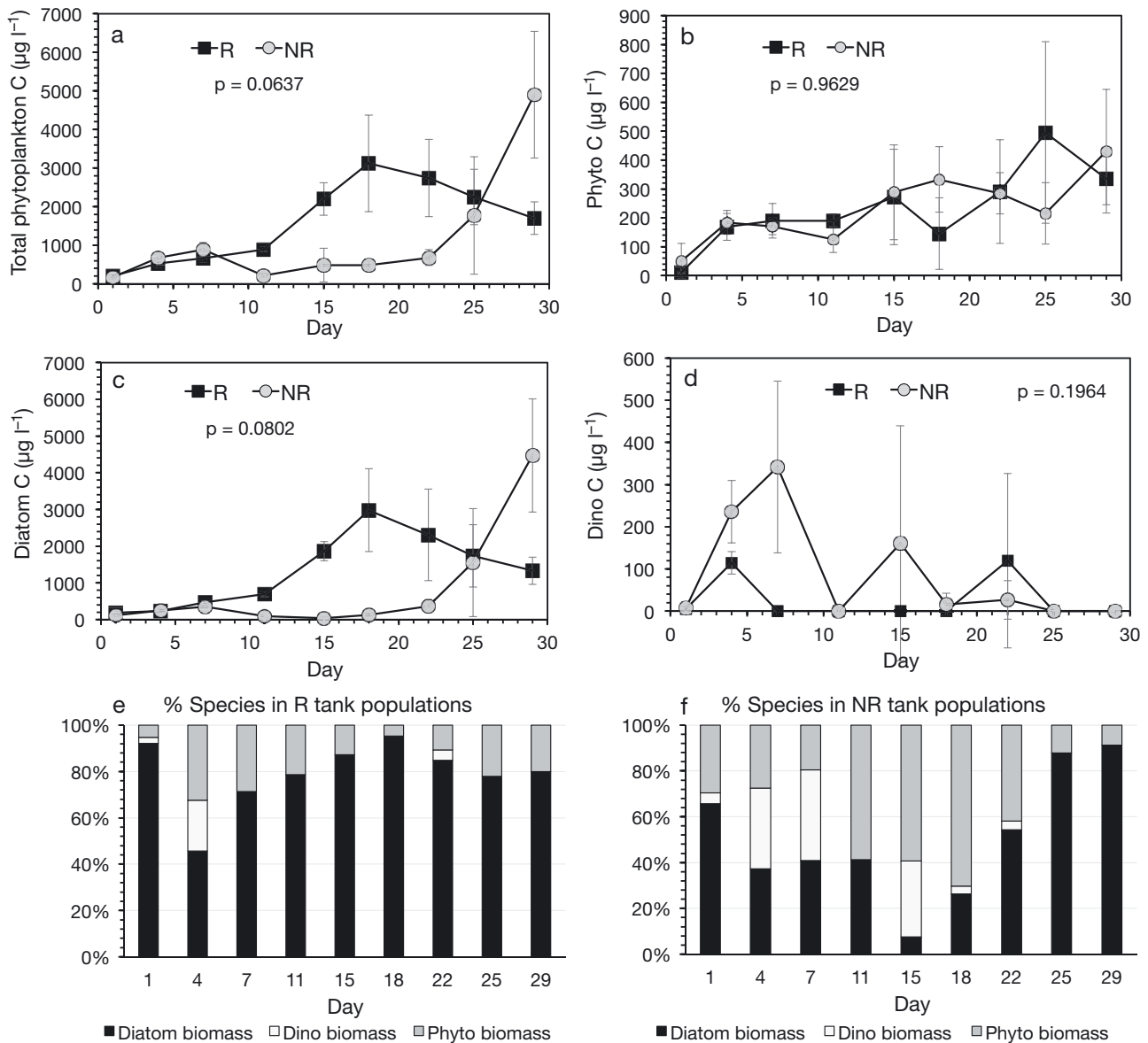
Fig. 3. (a) Total phytoplankton carbon (C; determined from direct cell counts after Strathman 1967), (b) phytoflagellate (phyto) carbon, (c) diatom carbon, (d) dinoflagellate (dino) carbon in resuspension tanks (R) and non-resuspension tanks (NR) over the experiment. Statistical difference is indicated (p ≤ 0.05). Percent species composition in (e) R tanks and (f) in NR tanks over the course of the experiment. All tanks received a daily addition of oyster biodeposits. Means ± SD, n = 3 per system

they each also had a significant time × treatment interaction as determined by repeated measures analysis (Tables 2d & S2d). Ammonium concentrations were significantly higher in NR tanks (5.8 ± 3.7 µmol l^{-1}) than in R tanks (1.47 ± 0.02 µmol l^{-1}) (p < 0.0001; Fig. 5a, Table 2d). SRP concentrations (Fig. 5b) were significantly higher in R tanks (1.46 ± 0.47 µmol l^{-1}) than in NR tanks (1.21 ± 0.63 µmol l^{-1}) (p = 0.0373; Fig. 5a, Table 2d) and were never limiting (i.e. <0.1 µmol l^{-1}; Fisher et al. 1992). SRP concentrations decreased significantly in NR tanks (p = 0.0038) from Day 11 to the end of the experiment but not over the

entire experiment. In R tanks there was no relationship with time. CDOM absorbance at 440 nm was significantly higher in NR tanks (0.044 ± 0.004 m^{-1}) than in R tanks (0.037 ± 0.003 m^{-1}) (p = 0.0005; Fig. S3g, Table S2d).

A significant time × treatment interaction was found for dissolved silicate, TDP, and the TN:TP ratio, although treatment was non-significant (Table 2d,e). The dissolved silicate concentration was similar in R and NR tanks (p = 0.5208; Fig. 5e, Table 2d); it decreased significantly over time in NR tanks (p = 0.0023) but not in R tanks (p = 0.1047). The TN:TP
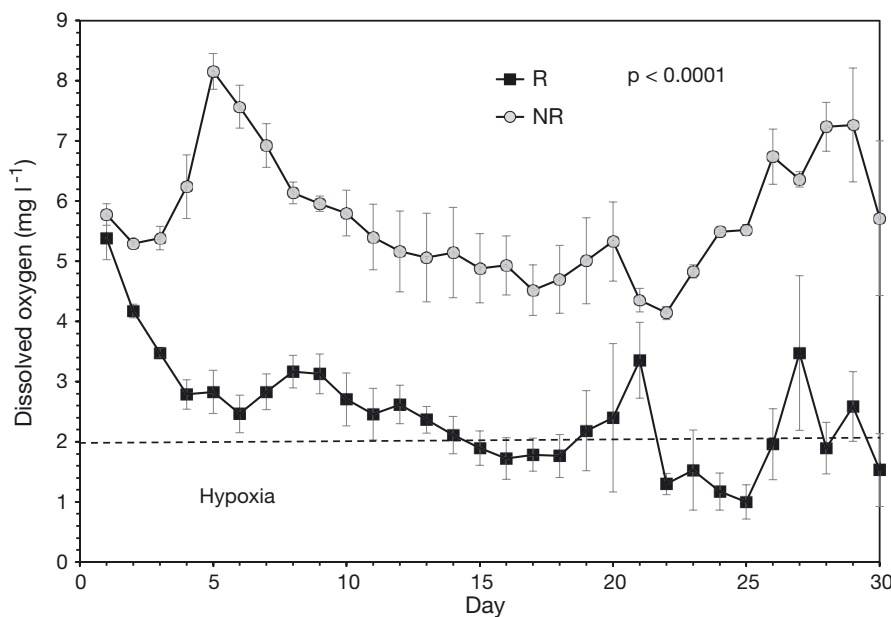
Fig. 4. Mean (±SD) water column dissolved oxygen concentrations in resuspension tanks (R) and non-resuspension tanks (NR) over the experiment, n = 3 for each system. All tanks received a daily addition of oyster biodeposits. Statistical significance is indicated (p ≤ 0.05). Dashed line: threshold for hypoxia (see Section 3.4)

ratio was similar in NR and R tanks (p = 0.0876; Fig. S3e, Table 2e); it increased significantly over time in NR tanks (p = 0.0472) but not in R tanks (p = 0.0966). Dissolved silicate concentrations ranged from about 120–60 µmol l⁻¹ over the experiment and silicate was not limiting, i.e. <5 µmol l⁻¹ (Fisher et al. 1992), in any of the systems. While TDP concentrations were similar in NR and R tanks (p = 0.4937; Fig. S3a, Table 2d), they decreased significantly over time in R tanks (p = 0.0484) but not in NR tanks (p = 0.2100).

TDN concentrations were similar in R and NR tanks (p = 0.2584; Fig. S3a, Table 2d). DIN:SRP ratios (p = 0.3814) and ratios of dissolved silicate to SRP (p = 0.0784) were similar between R and NR tanks (Table 2d), and there was no significant interaction of time × treatment (Table 2d).

3.5. Light penetration, microphytobenthos

Light, as measured by a homemade Secchi disk, penetrated 29.94 ± 8.41 cm into R tanks during resuspension and 68.35 ± 22.79 cm in NR tanks during mixing-on (p < 0.0001; Fig. 6a, Table 2f). During mixing-off, Secchi depth reached between 59.52 ± 10.96 cm in R tanks and 65.75 ± 22.85 cm in NR tanks (p = 0.0003; Fig. 6a, Table 2f).

Measured bottom irradiance levels during the resuspension phase were low in R tanks (0.1 ± 0.24 µmol m⁻² s⁻¹) due to high turbidities as a result

of high TSS and biodeposit resuspension (Figs. 1f & 2) and were significantly higher in NR tanks (41.79 ± 25.56 µmol m⁻² s⁻¹) (p < 0.0001; Fig. 6b, Table 2f). Irradiance at the bottom was similar between R tanks during mixing-off and NR tanks during mixing-on and -off (Fig. 6b).

Geometric mean irradiance in the water column during mixing-on was higher in NR tanks (121.39 ± 61.9 µmol m⁻² s⁻¹) than in R tanks (2.85 ± 3.76 µmol m⁻² s⁻¹) (p = 0.0009), which had higher resuspended TSS concentrations. A similar amount of light reached into R tanks during mixing-off as reached into NR tanks during mixing-on and mixing-off. Significantly more light reached into NR tanks than R tanks with mixing-on and -off combined, as determined with a Student-Newman-Keuls test in SAS v.8.2 (p ≤ 0.05).

Microphytobenthos grew on the sediment bottoms of R tanks, despite high bottom shear stress (~0.36–0.51 Pa during mixing-on phases); there was no light limitation in R tanks during mixing-off. Sediment chl a concentrations were similar in R and NR tanks (p = 0.6831; Table 2g, Fig. S2b). Gross dissolved oxygen production (dissolved oxygen flux in the light minus dissolved oxygen flux in the dark) indicated an active microphytobenthos in both tanks (p = 0.3148; Fig. S5a). While sediment chlorophyllide concentrations were significantly higher in NR than R tanks (p = 0.0172; Table 2g, Fig. S5c), sediment phaeophytin concentrations were similar (p = 0.3787; Table 2g), and variability in R tanks was high.
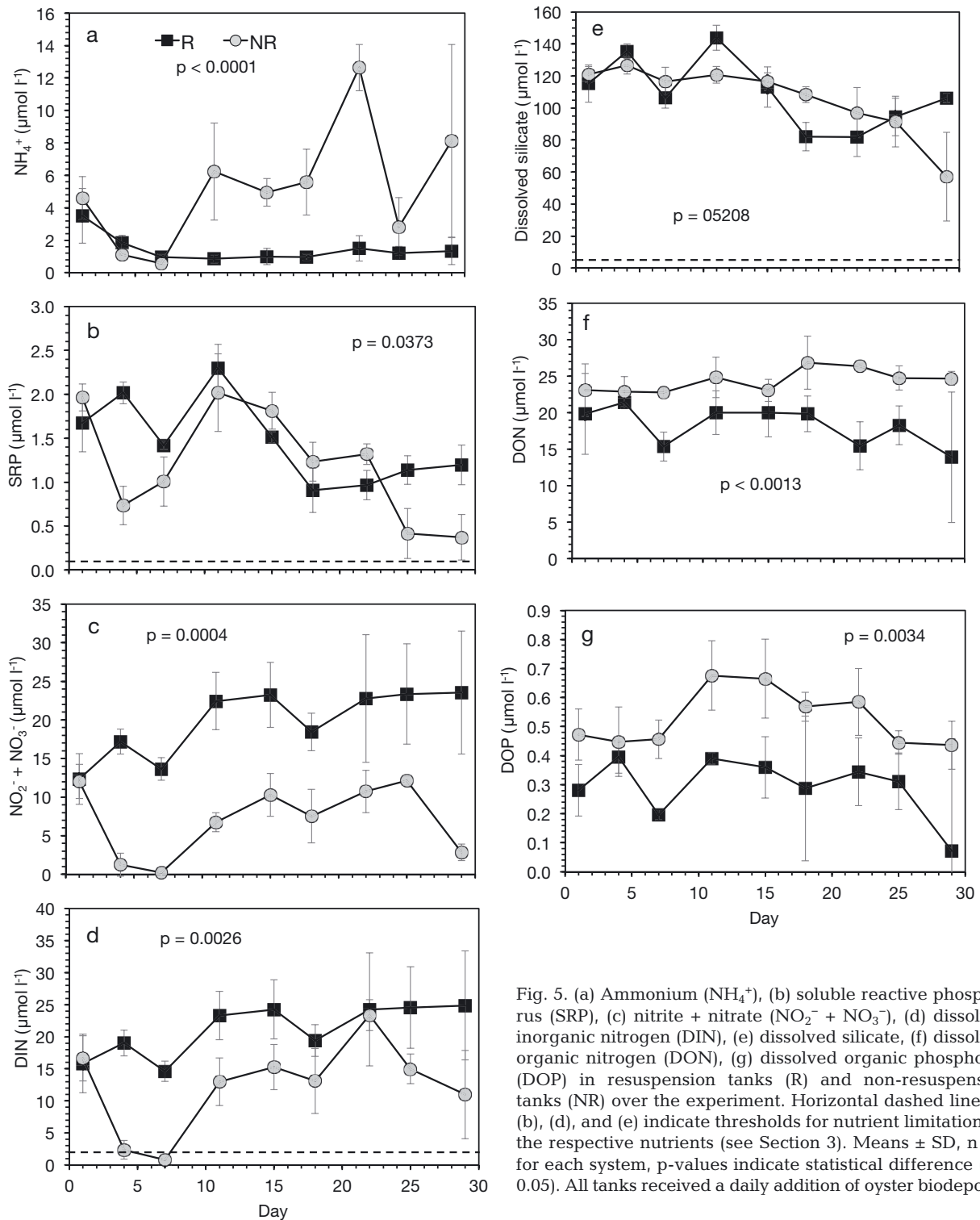
Fig. 5. (a) Ammonium (NH_4^+), (b) soluble reactive phosphorus (SRP), (c) nitrite + nitrate ($NO_2^- + NO_3^-$), (d) dissolved inorganic nitrogen (DIN), (e) dissolved silicate, (f) dissolved organic nitrogen (DON), (g) dissolved organic phosphorus (DOP) in resuspension tanks (R) and non-resuspension tanks (NR) over the experiment. Horizontal dashed lines in (b), (d), and (e) indicate thresholds for nutrient limitation for the respective nutrients (see Section 3). Means ± SD, n = 3 for each system, p-values indicate statistical difference (p ≤ 0.05). All tanks received a daily addition of oyster biodeposits

3.6. Sediment nutrient and gas fluxes

The dark sediment oxygen influx of 1198 ± 113 µmol m^{-2} h^{-1} in the NR tanks was more than twice as high as the R tank influx of about 516 ± 107 µmol m^{-2} h^{-1} (Fig. 7a). In the light, the sediment oxygen influx of 940 ± 237 µmol m^{-2} h^{-1} in NR tanks was about 3 times as high as the sediment oxygen influx of about 366 ± 20 µmol m^{-2} h^{-1} in R tanks (Fig. 7a). Dark compared to light fluxes were not significantly different for the respective treatments. Ammonium effluxes in the dark in NR tanks (104 ± 79 µmol m^{-2} h^{-1}) were
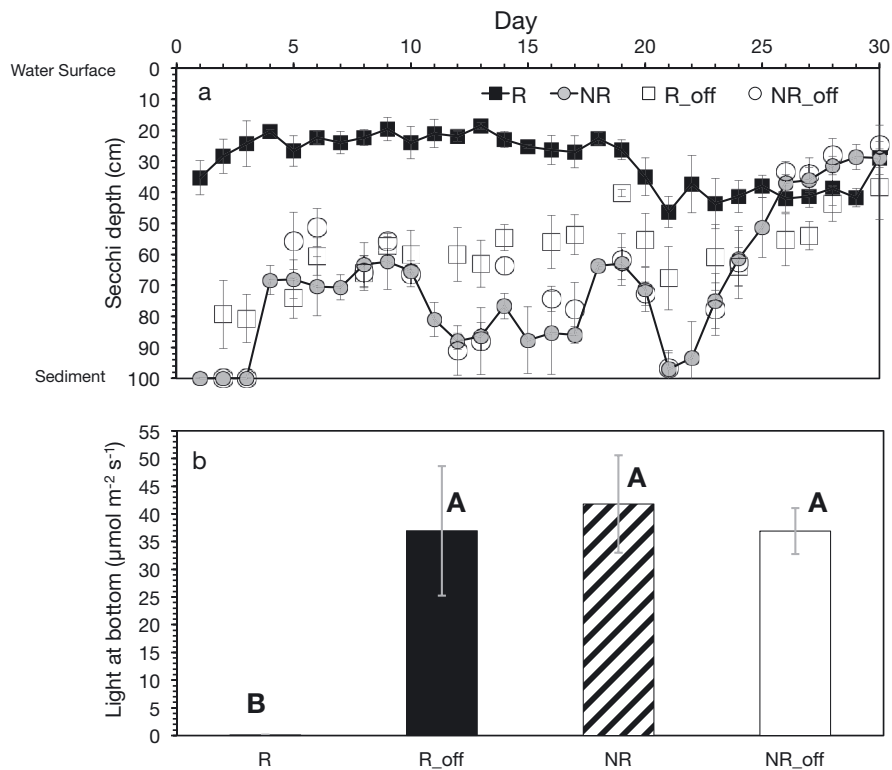
Fig. 6. (a) Mean (±SD) Secchi depth measured in in resuspension tanks (R) and in non-resuspension tanks (NR) during the mixing-on and mixing-off phases over the experiment. (b) Mean (±SD) irradiance at the bottom (photosynthetically active radiation, downwelling attenuation; LiCor light meter) calculated at the sediment surface during mixing-on and -off in resuspension (R) tanks and in non-resuspension (NR) tanks. Different letters indicate statistical differences (p ≤ 0.05); n = 3 for each system. All tanks received a daily addition of oyster biodeposits

significantly less than in R tanks (10 ± 50 µmol m^{-2} h^{-1}) (Fig. 7b). In the light, ammonium uptake was similar in NR and R tanks (Fig. 7b). Dark versus light ammonium fluxes were significantly different in NR tanks but not in R tanks (Fig. 7b). Nitrate plus nitrite fluxes were similar in the R tanks and NR tanks (63–129 µmol m^{-2} h^{-1}) and under illumination (~35 to ~82 µmol m^{-2} h^{-1}; Fig. 7c). Nitrate plus nitrite flux rates were significantly different in the dark compared to the light for both respective treatments (Fig. 7c). The dark R tank SRP effluxes averaged 22 ± 8 µmol m^{-2} h^{-1} while the NR tanks had an influx of 5 ± 5 µmol m^{-2} h^{-1} SRP, with the differences significant (Fig. 7d). In the light, R tank influxes of 31 ± 9 µmol m^{-2} h^{-1} SRP were significantly higher than the NR tank effluxes (7 ± 9 µmol m^{-2} h^{-1}; Fig. 7d). Only in the R tanks were the dark versus light fluxes significant. Sediment dinitrogen effluxes (81–241 µmol m^{-2} h^{-1}) were similar across all treatments, in the light and dark (Fig. 7e). In both R and NR tanks, dark effluxes of 139–167 µmol m^{-2} h^{-1} for DIN were similar (Fig. 7f). Light uptake of DIN was significantly higher in NR tanks (170 ± 40 µmol m^{-2} h^{-1}) than in R tanks ($51 \pm$

41 µmol m^{-2} h^{-1}) (Fig. 7f). DIN effluxes in the dark were significantly different from DIN uptake in the light, for both R and NR tanks (Fig. 7f).

Daily sediment uptake of dissolved oxygen was significantly higher in NR tanks (25.1 ± 4.1 mmol m^2 d^{-1}) than in R tanks (10.3 ± 0.8 mmol m^2 d^{-1}) (p = 0.0251; Fig. 7a). Daily uptake of ammonium was similar in R tanks (118 ± 767 µmol m^2 d^{-1}) and NR tanks (225 ± 219 µmol m^2 d^{-1}) (p = 0.8391; Fig. 7b). Denitrification rates were high and variable and not significantly different in R tanks (4422 ± 4850 µmol m^2 d^{-1}) and NR tanks (2513 ± 785 µmol m^2 d^{-1}) (p = 0.5703; Fig. 7e). While not significant (p = 0.0616), a trend (0.1 > p > 0.05) of a daily efflux of 771 ± 691 µmol m^2 d^{-1} of nitrate plus nitrite in R tanks compared to a daily uptake of 545 ± 365 µmol m^2 d^{-1} of nitrate plus nitrite in NR tanks was observed (Fig. 7c). While also not significant (p = 0.0564), a trend of a daily uptake of 215 ± 62 µmol m^2 d^{-1} of SRP in R tanks compared to a daily efflux of 53 ± 141 µmol m^2 d^{-1} of SRP in NR tanks was observed (Fig. 7d).

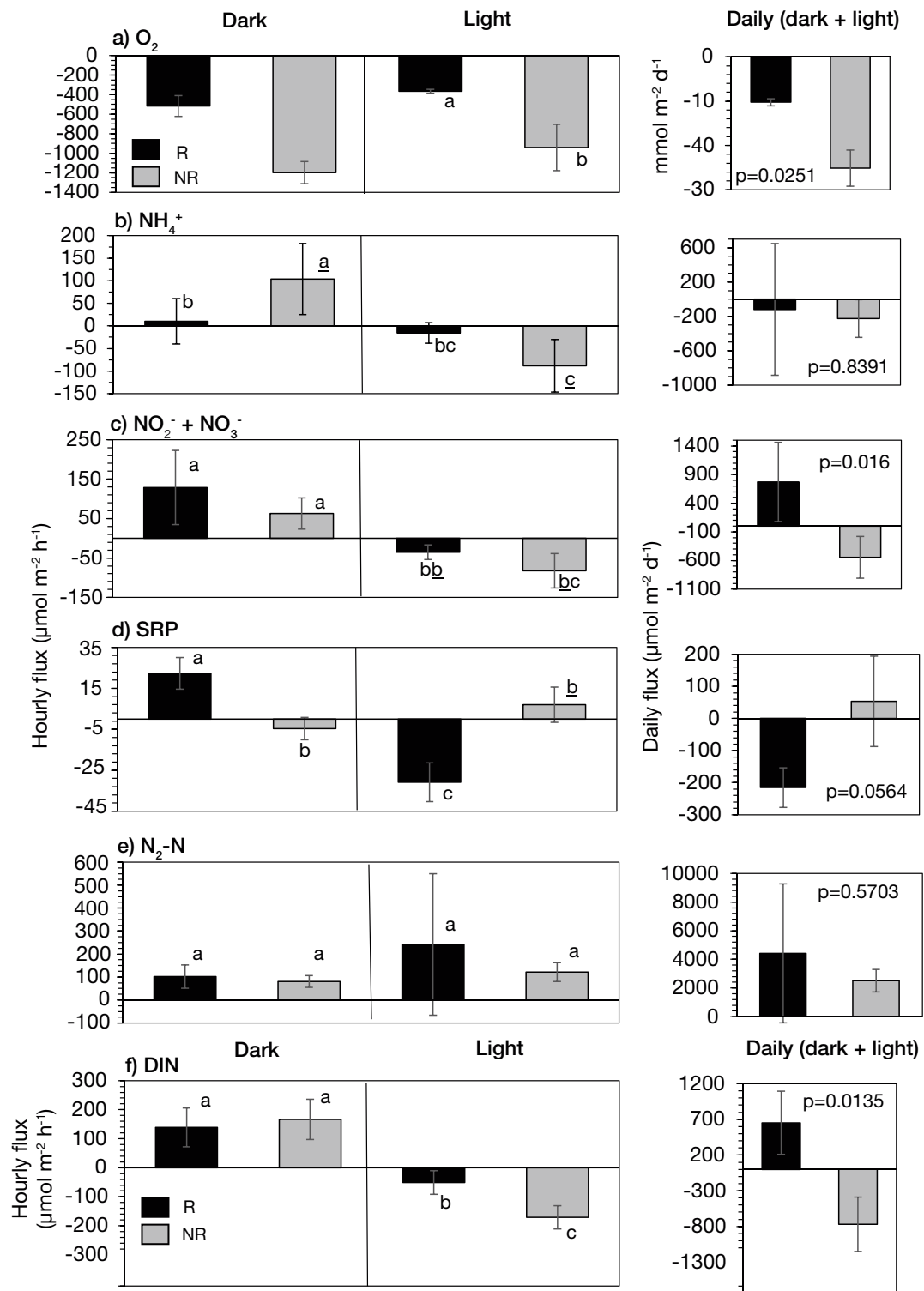Concentrations of carbon (3.66–3.72%), nitrogen (0.47–0.48%), phosphorus (0.09–0.1%), and

Fig. 7. Mean (±SD) sediment (a) oxygen (O_2) (b) ammonium (NH_4^+), (c) nitrite + nitrate ($NO_2^- + NO_3^-$), (d) soluble reactive phosphorus (SRP), (e) dinitrogen gas (N_2–N) and (f) dissolved inorganic nitrogen (DIN) fluxes from sediment cores collected from resuspension tanks (R) and non-resuspension tanks (NR); fluxes are mediated by microphytobenthos photosynthesis. All tanks had received 29 d of daily oyster biodeposit additions. Sediment fluxes were run in the dark and light; daily fluxes were calculated after Owens & Cornwell (2016). Different letters indicate statistical difference ($p < 0.05$), underscoring indicates trends ($p = 0.05–0.1$); $n = 3$ tanks system^{-1} with 2 cores per tank run
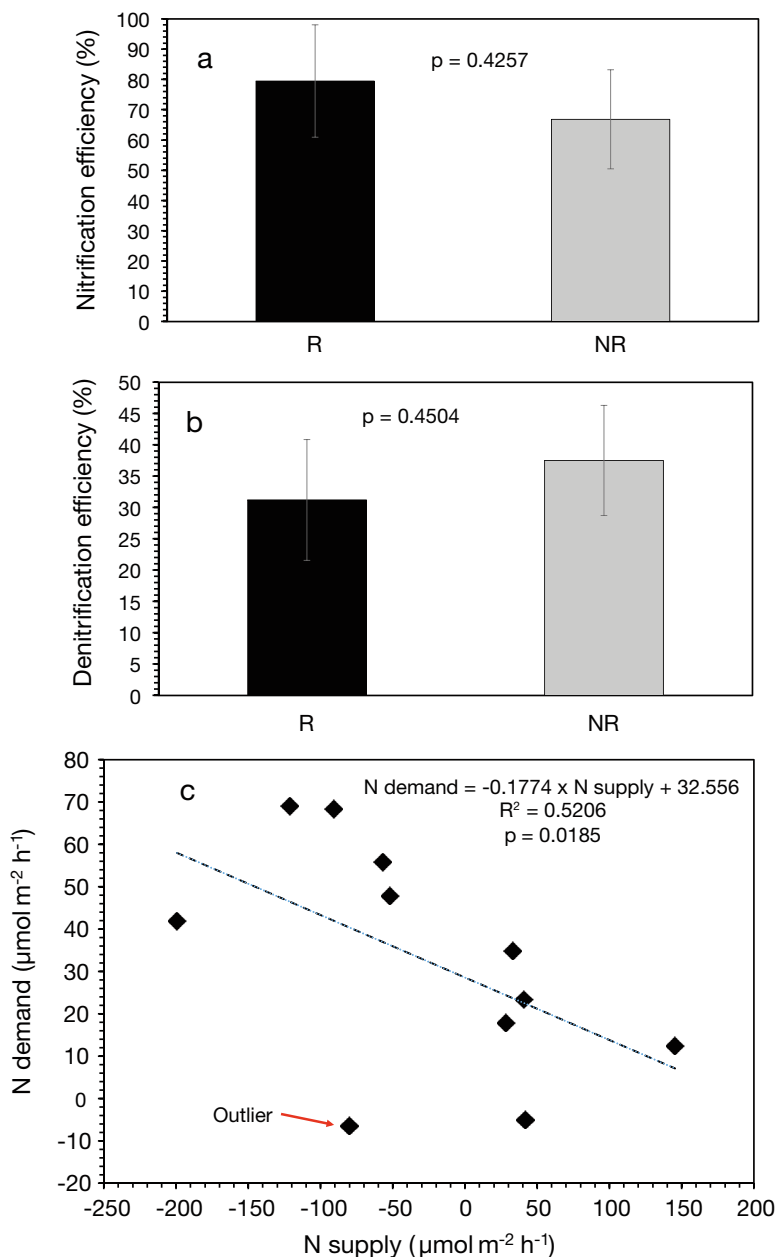
Fig. 8. Mean (±SD) (a) sediment nitrification efficiency and (b) sediment denitrification efficiency in resuspension (R) and non-resuspension (NR) tanks, n = 3 for each system. (c) Nitrogen (N) demand (defined as gross O_2 production = [O_2 in the light – O_2 in the dark] / 6.625) versus N supply (defined as NH_4^+ + NO_2^- + NO_3^- + N_2N, all in the light) measured in all individual sediment cores taken from all mesocosms at the end of the experiment. For the regression, one outlier was removed. Significance of the regression at the p ≤ 0.05 level. All tanks received a daily addition of oyster biodeposits

Sediment nitrification efficiency (%) is an estimate of the likelihood that ammonium is transferred to nitrate plus nitrite (Kellogg et al. 2013). Nitrification efficiencies were high and similar in R tanks (79.27 ± 18.55%) and NR tanks (66.82 ± 16.36%) (p = 0.4257; Fig. 8a). Denitrification efficiencies were moderate (31.23 ± 9.65% in R tanks and 37.52 ± 8.79% in NR tanks) and not significantly different (p = 0.4504; Fig. 8b). Nitrogen demand (gross dissolved oxygen production = [O_2 flux in the light – O_2 flux in the dark] / 6.625) was especially high when the nitrogen supply (the sum of ammonium, nitrate plus nitrite, and dinitrogen gas) was low (Fig. 8c).

3.7. Conversion of biodeposit nitrogen into labile nitrogen under resuspension

Modeled biodeposit nitrogen diagenesis based on daily added biodeposit nitrogen in this experiment (using rates and proportions from Testa et al. 2015 and Brady et al. 2013) resulted in 58000 μmol of newly available nitrogen over the 30 d experiment through daily biodeposit additions (Fig. 9). In R tanks with biodeposit resuspension, ΣNO_x averaged 52868 ± 14547 μmol nitrogen, and most biodeposit nitrogen was converted into nitrate plus nitrite with little (−28304 ± 2229 μmol N) going into ΣNH_4 and ΣDON (6135 ± 9335 μmol N) over the course of the experiment (Fig. 9). In NR tanks, biodeposit nitrogen primarily went into ΣDON (26092 ± 1811 μmol N) and ΣNH_4 (13365 ± 4938 μmol N) but not into ΣNO_x (−2920 ± 1444 μmol N; Fig. 9). DIN sediment fluxes also indicate DIN uptake in NR tanks and DIN release in R tanks (p = 0.0135; Fig. 7f).

4. DISCUSSION

Although the resuspension and export of biodeposits from aquaculture footprints has an important effect on the net balance of nutrients and oxygen

water content (82–83%) in the top 0.5 cm of sediment were similar in the R and NR tanks (Table 2g). The concentrations of carbon, nitrogen, and phosphorus in the mesocosms were similar to previous observations.
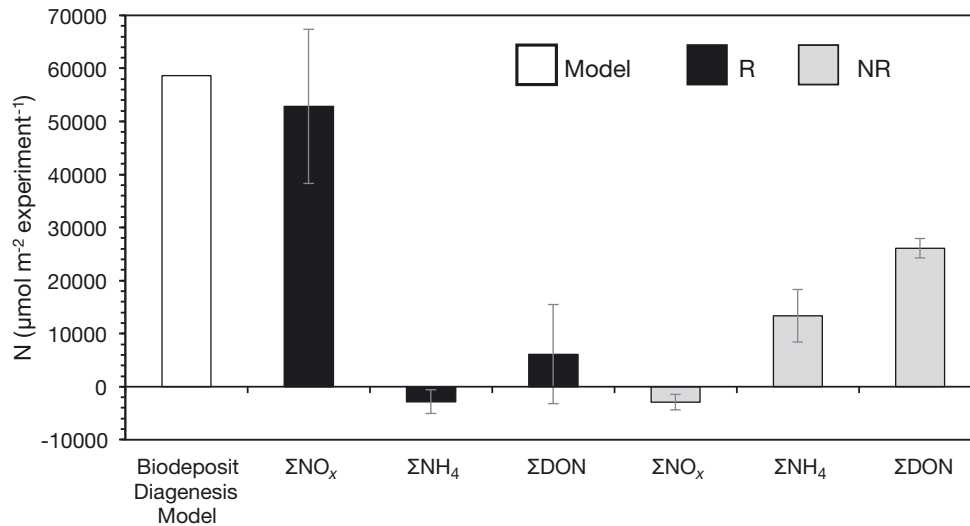
Fig. 9. Biodeposit nitrogen (N) diagenesis modeled based on daily added biodeposit N and using rates and proportions from Testa et al. (2015) and Brady et al. (2013), and cumulative nitrate + nitrite (ΣNO_x), ammonium (ΣNH_4), and dissolved organic nitrogen (ΣDON) in the water column in resuspension tanks (R) and non-resuspension tanks (NR) over the experiment. Means ± SD, n = 3 for each system. All tanks received a daily addition of oyster biodeposits. With biodeposit resuspension, biodeposit N in R tanks is primarily converted to water column nitrate + nitrite

(Gadeken et al. 2021), this study is the first to examine these processes under differential bottom shear stress regimes. As expected, biodeposits added to the low shear stress tanks (NR) remained on the bottom, while biodeposits in the high shear stress tanks (R) were resuspended, adding POM to the water column and inducing nitrification. In NR tanks, biogeochemical processes occurred primarily in the sediments, whereas in R tanks, biogeochemical processes shifted towards the water column. Biogeochemical processes in the water column under resuspension, typically, are not studied.

Resuspended biodeposits changed water column nutrient and oxygen dynamics considerably. Resuspended biodeposits were remineralized in the water column, leading to nitrification (Fig. 9) and oxygen uptake. In R tanks, dissolved oxygen concentrations in the water column were 43% of concentrations in NR tanks, with hypoxic conditions on multiple occasions. Nitrification was enhanced in tanks with TSS resuspension, as illustrated by significantly higher nitrate and nitrite concentrations in R tanks relative to NR tanks. Similarly, TSS resuspension in the Seine River enhanced nitrification rates (Brion et al. 2000), with increased nitrification rates with higher TSS concentrations in river water coincident with increased bacterial populations (Xia et al. 2004, 2009). Resuspension of biodeposits yielded nitrate plus nitrite through nitrification in the water column of R tanks, while the conversion of biodeposits to DON and ammonium was evident in NR tanks. Shear stress

above the critical shear stress resuspends sediments (Porter et al. 2010) and biodeposits (Porter et al. 2018a) back into the water column, where resuspended organic material may be decomposed (Ståhlberg et al. 2006, Moriarty et al. 2018, 2021), increase hypoxia (Moriarty et al. 2018), or be transported away (Testa et al. 2015).

The high water column nitrate concentrations in R tanks suggest that water column denitrification in the R tanks could have been enhanced, but our experiments did not include these measurements. Resuspended particles can enhance denitrification (Liu et al. 2013, Xia et al. 2017a, Zhu et al. 2018), with smaller, organic-rich particles enhancing denitrification compared to larger particles (Jia et al. 2016, Xia et al. 2017b) or particles with less organic content (Yao et al. 2016). Biodeposits in this experiment added organic content to suspended matter in the R tanks. Water column denitrification under *in situ* resuspension with biodeposits warrants further investigation.

The shift in balance between sediment and water column organic matter decomposition was reflected in treatment differences in sediment dissolved oxygen and sediment DIN fluxes. In R tanks, daily sediment DIN effluxes were primarily composed of nitrate and nitrite, whereas a daily sediment DIN uptake was measured in NR tanks, with significant differences in DIN fluxes between the R and NR tanks. Dark and light sediment oxygen demand was ~3 times higher in NR tanks than in R tanks, indicating that organic matter mineralization was higher under non-

resuspension conditions. Gross oxygen production (dissolved oxygen flux in the light minus dissolved oxygen flux in the dark) indicated productive microphytobenthic communities in all tanks. The productive microphytobenthic community was unexpected in R tanks because even only moderately enhanced bottom shear stress can erode microphytobenthos (Porter et al. 2004a), and increased TSS concentrations in R tanks led to less light at the sediment surface during mixing-on. The microphytobenthic community changed nutrient transformations and regeneration, consistent with observations in other studies (Sundbäck & Granéli 1988, Sundbäck et al. 1991, 2000).

Enhanced bottom shear stress may have increased diffusive fluxes (Dade 1993), as R tanks had higher sediment DIN effluxes driven by high nitrate plus nitrite effluxes. An enhanced flux of oxygen into permeable sediments mediated by hydrodynamics (Ziebis et al. 1996, Huettel et al. 1998), and to a lesser known degree in non-permeable sediments (Booij et al. 1994) as used in this experiment, can lead to a change in sediment oxygenation and thus subsequent changes in nitrogen transformations. Here, shear-stress-mediated enhanced diffusive fluxes likely enhanced sediment nitrate plus nitrite effluxes in the R tanks.

Studies in stream sediments (O'Connor & Hondzo 2008a,b) suggest that an optimal range of shear velocities for enhancing denitrification occurs depending on environmental conditions (chemical, physical, microbiological). Sediment experiments have shown that POM, oxygen conditions, microphytobenthos abundance, and nitrate in the water column modify nitrogen transformations and regeneration (Caffrey et al. 1993, Enoksson 1993, Newell et al. 2002). The proportion of sediment inorganic nitrogen exchange occurring as denitrification was ~80% in R tank sediments and ~90% in NR tank sediments, with the sediment denitrification efficiency (%), an estimate of the likelihood that nitrate plus nitrite are transferred to N_2 gas (Kellogg et al. 2013), being similar in both tank treatments. Nitrogen demand was especially high when the nitrogen supply was low (Fig. 8c), and conversely, when nitrogen supply was high, nitrogen demand was low (p = 0.0185; Fig. 8c). Therefore, the microalgae were either nitrogen-limited or dependent on the pore water as a nitrogen source (Sundbäck et al. 2000). It is also possible that microphytobenthos and denitrification competed for nitrate plus nitrite. Denitrification in NR tanks may have been overestimated, as flux experiments were run with water column nitrate plus nitrite concentrations higher than in the water column of the NR tanks ($7.09 \pm 4.66\ \mu mol\ l^{-1}$). Microphytobenthos was

resuspended and settled in R tanks, as water column chl *a* concentrations were significantly lower during mixing-off. However, water column chl *a* concentrations were enhanced in NR tanks during mixing-off, driven by 2 NR tanks on the last sampling date.

While high biodeposition in low-flow areas can adversely affect sediments under aquaculture rafts (Cranford et al. 2007, Testa et al. 2015), moderate deposition can enhance denitrification (Newell et al. 2002, Lunstrum et al. 2018). High rates of ammonium flux can occur in sediments that underlie natural bivalve populations (Dame et al. 1989, 1991, Asmus & Asmus 1991, Dame & Libes 1993), but this effect was not observed in our experiment. The sediment nitrification efficiency (%) was 79.27 ± 18.55% in R tank sediments and 66.82 ± 16.36% in NR tank sediments (p = 0.4257) indicating that any ammonium in the system was efficiently transferred to nitrate plus nitrite in the sediments instead of being regenerated as ammonium.

While the focus of many studies is primarily on how oysters enhance the biogeochemically driven nitrogen removal from sediments and, in some cases, directly from the bivalves (Caffrey et al. 2016, Arfken et al. 2017), the results are widely variable (e.g. Piehler & Smyth 2011, Smyth et al. 2013, Kellogg et al. 2013, 2014 and references therein). Our biodeposit additions to mesocosms stimulated nitrification in the water column with resuspension, whereas in the non-resuspended case, observations showed increasing sediment oxygen demand and DIN uptake. For calculations of oyster environmental benefits, the fraction of deposited material that is resuspended must be determined to indicate the true environmental footprint (Cerco 2015). Furthermore, altered biogeochemical processes in the water column associated with biodeposit resuspension are important, as evident in this study. The role of biodeposit resuspension in the nitrogen cycle must be further understood to clarify the role of oyster-mediated denitrification (Ayvazian et al. 2021, Rose et al. 2021) in nutrient management.

While in previous work (Porter et al. 2020a), tidal resuspension and biodeposit additions funneled biodeposits from phytoplankton into zooplankton, the experimental data shown here indicate that phytoplankton and zooplankton concentrations were similar in R and NR tanks. As an exception, Cryptophyceae, as measured by HPLC, were more abundant in R tanks than in NR tanks, perhaps because they are able to absorb wavelengths not available to other algae using phycobiliproteins (Heidenreich & Richardson 2020). Diatoms were significantly more abundant

in R tanks than in NR tanks from Days 7–18 of the experiment as indicated by direct counts and HPLC, but the results of direct counts were not significant when all days were included in the analysis. From Days 22–29, diatom biomass greatly increased in 2 of 3 NR tanks and became the dominant phytoplankton in NR tanks, accompanied by an uptake of nitrate and nitrite, SRP, and dissolved silicate. R tanks had been dominated by diatoms throughout the experiment.

Short-term experiments are not capable of uncovering direct and indirect interactions driven by nutrient, phytoplankton, and mesozooplankton dynamics. Indirect effects have often been identified by accident when experiments produced unanticipated results (Wootton 2002). Moreover, the focus in this experiment was on resuspended sediments and resuspended biodeposits that are difficult to track in nature (Testa et al. 2015) and cannot be resuspended in typical experimental ecosystem experiments with low bottom shear stress (Doering et al. 1986, Porter et al. 2004b, 2010). The STURM facility (Porter et al. 2018b) allowed high bottom shear stress and realistic water column turbulence levels for benthic–pelagic coupling experiments (Porter et al. 2010, 2013, 2018a, 2020a,b). While oysters were not directly included in this experiment, bivalve filtration reduces phytoplankton biomass (Cloern 1982, Cohen et al. 1984, Porter et al. 2004a), and inclusion of oysters might have reduced total phytoplankton biomass. While it is generally assumed that oysters reduce seston and phytoplankton concentrations while ignoring biodeposits (Newell & Koch 2004), oyster reefs do not necessarily reduce water column particulates or impact phytoplankton or microphytobenthic biomass or productivity (Plutchak et al. 2010). Seston decreases (interpreted as depletion) are spatially variable (Grizzle et al. 2018) and the interplay between bottom shear stress with sediment and biodeposit resuspension and oysters requires consideration.

Resuspended biodeposits were not exported as they would be in nature, requiring further study to include the effects of particulate removal. There may be positive effects when biodeposits are transported away, limiting organic over-enrichment and improving sediment biogeochemistry (1) under reefs or aquaculture cages with organic matter removed and (2) outside of reefs/aquaculture with organic matter added. As noted by Lunstrum et al. (2018), site-specific conditions such as hydrodynamics (Giles et al. 2009) and water depth (Wilson & Vopel 2015) can influence the benthic footprint area, as shallower or high current sites can disperse (and thus dilute)

biodeposits over larger areas. While it is generally assumed that oyster biodeposits remain in oyster reefs (Newell et al. 2005, Kellogg et al. 2013), several studies suggest that biodeposits can be resuspended (Colden et al. 2016, Porter et al. 2018a, 2020) and transported by currents (Lund 1957, Widdows et al. 1998, Testa et al. 2015). STURM tanks are enclosed, but had the resuspended biodeposits been transported away, water column nutrient concentrations in R tanks would likely have been lower. The dynamics of biodeposit transport and the bivalve footprint area should be addressed in future studies.

Oysters and water flow affect benthic–pelagic coupling processes and the nitrogen cycle (Porter et al. 2004a). Presently, oyster aquaculture practices are considered a BMP for Chesapeake Bay, primarily due to nitrogen assimilation into oyster tissues which are then removed at harvest (i.e. bioextraction). However, oyster biodeposit resuspension must be considered when further evaluating oysters as a BMP for Chesapeake Bay or bivalves as a BMP elsewhere in the world to help control eutrophication, and should be included in physical–biological–biogeochemical models. Oyster biodeposits can be resuspended into the water column at intermediate shear stress where they can affect nutrient transformations, nutrient regeneration, and the nitrogen budget (Porter et al. 2018a). While we used oysters as our example here, this research applies to other bivalve species and eutrophic estuaries worldwide. Moreover, effects of biodeposit resuspension on water column biogeochemistry and potential denitrification under *in situ* resuspension should be investigated further to clarify the role of bivalve-mediated denitrification (Ayvazian et al. 2021, Rose et al. 2021) in nutrient management.

LITERATURE CITED

Almroth E, Tengberg A, Andersson JH, Pakhomova S, Hall POJ (2009) Effects of resuspension on benthic fluxes of oxygen, nutrients, dissolved inorganic carbon, iron and manganese in the Gulf of Finland, Baltic Sea. Cont Shelf Res 29:807–818

Almroth-Rosell E, Tengberg A, Andersson S, Apler A, Hall POJ (2012) Effects of simulated natural and massive resuspension on benthic oxygen, nutrient and dissolved inorganic carbon fluxes in Loch Creran, Scotland. J Sea Res 72:38–48

Arfken A, Song B, Bowman JS, Piehler M (2017) Denitrification potential of the eastern oyster microbiome using a 16S rRNA gene based metabolic inference approach. PLOS ONE 12:e0185071

Asmus RM, Asmus H (1991) Mussel beds: Limiting or promoting phytoplankton? J Exp Mar Biol Ecol 148:215–232

Ator SW, García AM, Schwarz GE, Blomquist JD, Sekellick AJ (2019) Toward explaining nitrogen and phosphorus trends in Chesapeake Bay tributaries, 1992–2012. J Am Water Resour Assoc 55:1149–1168

Ayvazian S, Mulvaney K, Zarnoch C, Palta M and others (2021) Beyond bioextraction: the role of oyster-mediated denitrification in nutrient management. Environ Sci Technol 55:14457–14465

Berg JA, Newell RIE (1986) Temporal and spatial variations in the composition of seston available to the suspension feeder *Crassostrea virginica.* Estuar Coast Shelf Sci 23:375–386

Beseres Pollack J, Yoskowitz D, Kim HC, Montagna PA (2013) Role and value of nitrogen regulation provided by oysters (*Crassostrea virginica*) in the Mission-Aransas Estuary, Texas, USA. PLOS ONE 8:e65314

Booij K, Sundby B, Helder H (1994) Measuring the flux of oxygen to a muddy sediment with a cylindrical microcosm. Neth J Sea Res 32:1–11

Brady DC, Testa JM, Di Toro DM, Boynton WR, Kemp WM (2013) Sediment flux modeling: calibration and application for coastal systems. Estuar Coast Shelf Sci 117:107–124

Bricker SB, Rice KC, Bricker OP (2014) From headwaters to coast: influence of human activities on water quality of the Potomac River Estuary. Aquat Geochem 20:291–323

Bricker SB, Grizzle RE, Trowbridge P, Rose JM and others (2020) Bioextractive removal of nitrogen by oysters in Great Bay Piscataqua River Estuary, New Hampshire, USA. Estuaries Coasts 43:23–38

Brion N, Billen G, Guezennec L, Ficht A (2000) Distribution of nitrifying activity in the Seine River (France) from Paris to the estuary. Estuaries 5:669–682

Caffrey JM, Sloth NP, Kaspar HF, Blackburn TH (1993) Effect of organic loading on nitrification and denitrification in a marine sediment microcosm. FEMS Microbiol Ecol 12:159–167

Caffrey JM, Hollibaugh JT, Mortazavi B (2016) Living oysters and their shells as sites of nitrification and denitrification. Mar Pollut Bull 112:86–90

Cerco CF (2015) A multi-module approach to calculation of oyster (*Crassostrea virginica*) environmental benefits. Environ Manage 56:467–479

Chen CC, Kemp WM (2004) Periphyton communities in experimental marine ecosystems: scaling the effects of removal from container walls. Mar Ecol Prog Ser 271:27–41

Chen CC, Petersen JE, Kemp WM (1997) Spatial and temporal scaling of periphyton growth on walls of estuarine mesocosms. Mar Ecol Prog Ser 155:1–15

Cloern JE (1982) Does the benthos control phytoplankton biomass in south San Francisco Bay? Mar Ecol Prog Ser 9:191–202

Cohen RRH, Dresler PV, Phillips EJP, Cory RL (1984) The effect of the Asiatic clam, *Corbicula fluminea*, on phytoplankton of the Potomac River, Maryland. Limnol Oceanogr 29:170–180

Colden AM, Fall KA, Cartwright GM, Friedrichs CT (2016) Sediment suspension and deposition across restored oyster reefs of varying orientation to flow: implications for restoration. Estuaries Coasts 39:1435–1448

Corbett DR (2010) Resuspension and estuarine nutrient cycling: insights from the Neuse River Estuary. Biogeosciences 7:3289–3300

Cranford PJ, Strain PM, Dowd M, Hargrave BT, Grant J, Archambault M (2007) Influence of mussel aquaculture on nitrogen dynamics in a nutrient enriched coastal embayment. Mar Ecol Prog Ser 347:61–78

Crawford SM, Sanford LP (2001) Boundary shear velocities and fluxes in the MEERC experimental ecosystems. Mar Ecol Prog Ser 210:1–12

Crowder MJ, Hand DJ (1990) Analysis of repeated measures. Chapman & Hall, London

Dade WB (1993) Near-bed turbulence and hydrodynamic control of diffusional mass transfer at the sea floor. Limnol Oceanogr 38:52–69

Dame RF, Libes S (1993) Oyster reefs and nutrient retention in tidal creeks. J Exp Mar Biol Ecol 171:251–258

Dame RF, Spurrier JD, Wolaver TG (1989) Carbon, nitrogen and phosphorus processing by an oyster reef. Mar Ecol Prog Ser 54:249–256

Dame RF, Spurrier JD, Williams TM, Kjerfve B and others (1991) Annual material processing by a salt marsh–estuarine basin in South Carolina, USA. Mar Ecol Prog Ser 72:153–166

Doering PH, Oviatt CA, Kelly JR (1986) The effects of the filter-feeding clam *Mercenaria mercenaria* on carbon cycling in experimental marine mesocosms. J Mar Res 44:839–861

Enoksson V (1993) Nutrient recycling by coastal sediments: effects of added algal material. Mar Ecol Prog Ser 92:245–254

Fisher TR, Peele ER, Ammerman JW, Harding LW Jr (1992) Nutrient limitation of phytoplankton in Chesapeake Bay. Mar Ecol Prog Ser 82:51–63

Gadeken K, Clemo WC, Ballentine W, Dykstra SL and others (2021) Transport of biodeposits and benthic footprint around an oyster farm, Damariscotta Estuary, Maine. PeerJ 9:e11862

Giles H, Broekhuizen N, Bryan KR, Pilditch CA (2009) Modelling the dispersal of biodeposits from mussel farms: the importance of simulating biodeposit erosion and decay. Aquaculture 291:168–178

Greenhouse SW, Geisser S (1959) On methods in the analysis of profile data. Psychometrika 24:95–112

Grizzle RE, Rasmussen A, Martignette AJ, Ward K, Coen LD (2018) Mapping seston depletion over an intertidal eastern oyster (*Crassostrea virginica*) reef: implications for restoration of multiple habitats. Estuar Coast Shelf Sci 212:265–272

Gust G (1988) Skin friction probes for field applications. J Geophys Res 93:14121–14132

Harding LW Jr, Mallonee ME, Perry ES, Miller WD, Adolf JE, Gallegos CL, Paerl HW (2019) Long-term trends, current status, and transitions of water quality in Chesapeake Bay. Sci Rep 9:6709

Haven DS, Morales-Alamo R (1970) Filtration of particles from suspension by the American oyster *Crassostrea virginica*. Biol Bull (Woods Hole) 139:248–264

Heidenreich KM, Richardson TL (2020) Photopigment, absorption, and growth responses of marine cryptophytes to varying spectral irradiance. J Phycol 56: 507–520

Higgins CB, Stephenson K, Brown BL (2011) Nutrient bioassimilation capacity of aquacultured oysters: quantification of an ecosystem service. J Environ Qual 40:271–277

Higgins CB, Tobias C, Piehler MF, Smyth AR, Dame RF, Stephenson K, Brown BL (2013) Effect of aquacultured oyster biodeposition on sediment N_2 production in Chesapeake Bay. Mar Ecol Prog Ser 473:7–27

Holmer M, Thorsen SW, Carlsson MS, Kjerulf PJ (2015) Pelagic and benthic nutrient regeneration processes in mussel cultures (*Mytilus edulis*) in a eutrophic coastal area (Skive Fjord, Denmark). Estuaries Coasts 38: 1629–1641

Huettel M, Ziebis W, Forster S, Luther GW (1998) Advective transport affecting metal and nutrient distributions and interfacial fluxes in permeable sediments. Geochim Cosmochim Acta 62:613–631

Hylén A, Taylor D, Kononets M, Lindegarth M, Stedt A, Bonaglia S, Bergstrom P (2021) *In situ* characterization of benthic fluxes and denitrification efficiency in a newly re-established mussel farm. Sci Total Environ 782: 146853

Isobe K, Ohte N (2014) Ecological perspectives on microbes involved in N-cycling. Microbes Environ 29:4–16

Jackson M, Owens MS, Cornwell JC, Kellogg ML (2018) Comparison of methods for determining biogeochemical fluxes from a restored oyster reef. PLOS ONE 13: e0209799

Jia Z, Liu T, Xia X, Xia N (2016) Effect of particle size and composition of suspended sediment on denitrification in river water. Sci Total Environ 541:934–940

Jordan SJ (1987) Sedimentation and remineralization associated with biodeposition by the American oyster *Crassostrea virginica*. PhD thesis, University of Maryland, College Park, MD

Kana TM, Darkangelo C, Hunt MD, Oldham JB, Bennett GE, Cornwell JC (1994) Membrane inlet mass spectrometer for rapid high-precision determination of N_2, O_2 and Ar in environmental water samples. Anal Chem 66:4166–4170

Kana TM, Sullivan MB, Cornwell JC, Groszkowski KM (1998) Denitrification in estuarine sediments determined by membrane inlet mass spectrometry. Limnol Oceanogr 43:334–339

Kellogg ML, Cornwell JC, Owens MS, Paynter KT (2013) Denitrification and nutrient assimilation on a restored oyster reef. Mar Ecol Prog Ser 480:1–19

Kellogg ML, Smyth AR, Luckenbach MW, Carmichael RH and others (2014) Use of oysters to mitigate eutrophica-

tion in coastal waters. Estuar Coast Shelf Sci 151: 156–168

Kemp WM, Boynton WR, Adolf JE, Boesch DF and others (2005) Eutrophication of Chesapeake Bay: historical trends and ecological interactions. Mar Ecol Prog Ser 303:1–29

Kotta J, Futter M, Kaasik A, Liversage K and others (2020) Cleaning up seas using blue growth initiatives: mussel farming for eutrophication control in the Baltic Sea. Sci Total Environ 709:136144

Lacouture RV (2010) Quality assurance documentation plan for the phytoplankton component of the Chesapeake Bay water quality monitoring program. Report prepared for the Maryland Department of Natural Resources by the Morgan State University Estuarine Research Center. https://www.chesapeakebay.net/documents/3684/md_phytoplankton_qapp_2009-2010.pdf

Lindahl O (2011) Mussel farming as a tool for re-eutrophication of coastal waters: experiences from Sweden. In: Shumway SE (ed) Shellfish aquaculture and the environment. Wiley Blackwell, Oxford, p 217–237

Liu T, Xia X, Liu S, Mou X, Qiu Y (2013) Acceleration of denitrification in turbid rivers due to denitrification occurring on suspended sediment in oxic waters. Environ Sci Technol 47:4053–4061

Lund EJ (1957) Self silting, survival of the oyster as a closed system and reducing tendencies of the environment of the oyster. Publ Inst Mar Sci Univ Tex 4:313–319

Lunstrum A, McGlathery K, Smyth A (2018) Oyster (*Crassostrea virginica*) aquaculture shifts sediment nitrogen processes toward mineralization over denitrification. Estuaries Coasts 41:1130–1146

Marshall HG, Alden RW (1990) Spatial and temporal diatom assemblages and other phytoplankton within the lower Chesapeake Bay, USA. In: Simola H (ed) Proc 10th Int Diatom Symposium. Koeltz Scientific Books, Koenigstein, p 311–322

Moriarty JM, Harris CK, Friedrichs MAM, Fennel K, Xu K (2018) Impact of seabed resuspension on oxygen and nitrogen dynamics in the Northern Gulf of Mexico: a numerical modeling study. J Geophys Res 123: 7237–7263

Moriarty JM, Friedrichs MAM, Harris CK (2021) Seabed resuspension in the Chesapeake Bay: implications for biogeochemical cycling and hypoxia. Estuaries Coasts 44:103–122

Murphy AE, Emery KA, Anderson IC, Pace ML, Brush MJ, Rheuban JE (2016) Quantifying the effects of commercial clam aquaculture on C and N cycling: an integrated ecosystem approach. Estuaries Coasts 39:1746–1761

Murphy RR, Perry E, Harcum J, Keisman J (2019) A generalized additive model approach to evaluating water quality: Chesapeake Bay case study. Environ Model Softw 118:1–13

Newell RIE (1988) Ecological changes in Chesapeake Bay: Are they the result of overharvesting the American oyster, *Crassostrea virginica*? In: Lynch MP, Krome EC (eds) Understanding the estuary: advances in Chesapeake Bay research. Publication No. 129 (CBP/TRS 24/88). Chesapeake Research Consortium, Gloucester Point, VA, p 536–546

Newell RIE, Koch EW (2004) Modeling seagrass density and distribution in response to changes in turbidity stemming from bivalve filtration and seagrass sediment stabilization. Estuaries 27:793–806

Newell R, Langdon CJ (1996) Mechanisms and the physiology of larval and adult feeding. In: Kennedy VS, Newell RIE, Eble AF (eds) The eastern oyster *Crassostrea virginica*. Maryland Sea Grant, College Park, MD, p 185−229

Newell RIE, Cornwell JC, Owens MS (2002) Influence of simulated bivalve biodeposition and microphyto benthos on sediment nitrogen dynamics: a laboratory study. Limnol Oceanogr 47:1367−1379

Newell RIE, Fisher TR, Holyoke RR, Cornwell JC (2005) Influence of eastern oysters on nitrogen and phosphorus regeneration in Chesapeake Bay, USA. In: Dame RF, Olenin S (eds) The comparative roles of suspension feeders in ecosystems, Vol 47. Kluwer, Dordrecht, p 93−120

O'Connor BL, Hondzo M (2008a) Enhancement and inhibition of denitrification by fluid-flow and dissolved oxygen flux to stream sediments. Environ Sci Technol 42: 119−125

O'Connor BL, Hondzo M (2008b) Response to comment on 'Enhancement and inhibition of denitrification by fluid-flow and dissolved oxygen flux to stream sediments'. Environ Sci Technol 42:8611−8612

Owens MS, Cornwell JC (2016) The benthic exchange of O_2, N_2 and dissolved nutrients using small core incubations. J Vis Exp 114:e54098

Petersen JE, Sanford LP, Kemp WM (1998) Coastal plankton responses to turbulent mixing in experimental ecosystems. Mar Ecol Prog Ser 171:23−41

Petersen JK, Saurel C, Nielsen P, Timmermann K (2016) The use of shellfish for eutrophication control. Aquacult Int 24:857−878

Piehler MF, Smyth AR (2011) Habitat-specific distinctions in estuarine denitrification affect both ecosystem function and services. Ecosphere 2:art12

Plutchak R, Major K, Cebrian J, Foster CD and others (2010) Impacts of oyster reef restoration on primary productivity and nutrient dynamics in tidal creeks of the north central Gulf of Mexico. Estuaries Coasts 33:1355−1364

Porter ET, Sanford LP, Suttles SE (2000) Gypsum dissolution is not a universal integrator of 'water motion'. Limnol Oceanogr 45:145−158

Porter ET, Cornwell JC, Sanford LP, Newell RIE (2004a) Effect of oysters *Crassostrea virginica* and bottom shear velocity on benthic−pelagic coupling and estuarine water quality. Mar Ecol Prog Ser 271:61−75

Porter ET, Sanford LP, Gust G, Porter FS (2004b) Combined water-column mixing and benthic boundary-layer flow in mesocosms: key for realistic benthic−pelagic coupling studies. Mar Ecol Prog Ser 271:43−60

Porter ET, Owens M, Cornwell JC (2006) Effect of sediment manipulation on the biogeochemistry of experimental sediment systems. J Coast Res 22:1539−1551

Porter ET, Mason RP, Sanford LP (2010) Effect of tidal resuspension on benthic−pelagic coupling in an experimental ecosystem study. Mar Ecol Prog Ser 413:33−53

Porter ET, Mason RP, Sanford LP (2013) Effects of shear stress and hard clams on seston, microphytobenthos, and nitrogen dynamics in mesocosms with tidal resuspension. Mar Ecol Prog Ser 479:25−46

Porter ET, Franz H, Lacouture R (2018a) Impact of eastern oyster *Crassostrea virginica* biodeposit resuspension on the seston, nutrient, phytoplankton, and zooplankton dynamics: a mesocosm experiment. Mar Ecol Prog Ser 586:21−40

Porter ET, Sanford LP, Porter FS, Mason RP (2018b) STURM: resuspension mesocosms with realistic bottom shear stress and water column turbulence for benthic−pelagic coupling studies: design and applications. J Exp Mar Biol Ecol 499:35−50

Porter ET, Robins E, Davis S, Lacouture R, Cornwell J (2020a) Effects of resuspension of eastern oyster *Crassostrea virginica* biodeposits on phytoplankton community structure. Mar Ecol Prog Ser 640:79−105

Porter ET, Johnson BJ, Sanford LP (2020b) Effects of hard clam (*Mercenaria mercenaria*) density and bottom shear stress on cohesive sediment erodibility and implications for benthic−pelagic coupling. J Mar Res 78:91−130

Qin B, Hu W, Gao G, Luo L, Zhang J (2004) Dynamics of sediment resuspension and the conceptual schema of nutrient release in the large shallow Lake Taihu, China. Chin Sci Bull 49:54−64

Ray NE, Li J, Kangas PC, Terlizzi DE (2015) Water quality upstream and downstream of a commercial oyster aquaculture facility in Chesapeake Bay, USA. Aquacult Eng 68:35−42

Reidenbach MA, Berg P, Hume A, Hansen JCR, Whitman ER (2013) Hydrodynamics of intertidal oyster reefs: the influence of boundary layer flow processes on sediment and oxygen exchange. Limnol Oceanogr Fluids Environ 3:225−239

Ritzenhofen L, Buer AL, Gyraite G, Dahlke S, Klemmstein A, Schernewski G (2021) Blue mussel (*Mytilus* spp.) cultivation in mesohaline eutrophied inner coastal waters: mitigation potential, threats and cost effectiveness. PeerJ 9: e11247

Rosa M, Ward JE, Shumway SE (2018) Selective capture and ingestion of particles by suspension-feeding bivalve molluscs: a review. J Shellfish Res 37:727−746

Rose JM, Bricker SB, Tedesco MA, Wikfors GH (2014) A role for shellfish aquaculture in coastal nitrogen management. Environ Sci Technol 48:2519−2525

Rose JM, Gosnell JS, Bricker S, Brush MJ and others (2021) Opportunities and challenges for including oyster-mediated denitrification in nitrogen management plans. Estuaries Coasts 44:2041−2055

Sanford LP (1997) Turbulent mixing in experimental ecosystems. Mar Ecol Prog Ser 161:265−293

Schulte DM, Burke RP (2014) Recruitment enhancement as an indicator of oyster restoration success in Chesapeake Bay. Ecol Restor 32:434−440

Smyth AR, Geraldi NR, Piehler MF (2013) Oyster-mediated benthic−pelagic coupling modifies nitrogen pools and processes. Mar Ecol Prog Ser 493:23−30

Smyth AR, Murphy AE, Anderson IC, Song B (2018) Differential effects of bivalves on sediment nitrogen cycling in a shallow coastal bay. Estuaries Coasts 41:1147−1163

Ståhlberg C, Bastviken D, Svensson BH, Rahm L (2006) Mineralisation of organic matter in coastal sediments at different frequency and duration of resuspension. Estuar Coast Shelf Sci 70:317−325

Strathmann RR (1967) Estimating the organic carbon content of phytoplankton from cell volume or plasma volume. Limnol Oceanogr 12:411−418

Sundbäck K, Granéli W (1988) Influence of microphytobenthos on the nutrient flux between sediment and water: a laboratory study. Mar Ecol Prog Ser 43:63−69

Sundbäck K, Enoksson V, Granéli W, Pettersson K (1991) Influence of sublittoral microphytobenthos on the oxygen and nutrient flux between sediment and water: a

laboratory continuous-flow study. Mar Ecol Prog Ser 74: 263–279

Sundbäck K, Miles A, Göransson E (2000) Nitrogen fluxes, denitrification and the role of microphytobenthos in microtidal shallow-water sediments: an annual study. Mar Ecol Prog Ser 200:59–76

Tennekes H, Lumley JL (1972) A first course in turbulence. MIT Press, Cambridge, MA

Testa JM, Brady DC, Cornwell JC, Owens MS and others (2015) Modeling the impact of floating oyster (*Crassostrea virginica*) aquaculture on sediment–water nutrient and oxygen fluxes. Aquacult Environ Interact 7: 205–222

Utermöhl H (1958) Zur Vervollkommnung der quantitativen Phytoplankton-Methodik. Mitt Int Ver Theor Angew Limnol 9:1–38

Van Heukelem L, Thomas CS (2001) Computer-assisted high-performance liquid chromatography method development with applications to the isolation and analysis of phytoplankton pigments. J Chromatogr A 910:31–49

Vaquer-Sunyer R, Duarte CM (2008) Thresholds of hypoxia for marine biodiversity. Proc Natl Acad Sci USA 105: 15452–15457

Wainright SC (1987) Stimulation of heterotrophic microplankton production by resuspended marine sediments. Science 238:1710–1712

Wainright SC (1990) Sediment-to-water fluxes of particulate material and microbes by resuspension and their contribution to the planktonic food web. Mar Ecol Prog Ser 62: 271–281

White JR, Roman MR (1992) Seasonal study of grazing by metazoan zooplankton in the mesohaline Chesapeake Bay. Mar Ecol Prog Ser 86:251–261

Widdows J, Brinsley MD, Elliott M (1998) Use of an *in situ* flume to quantify particle flux (biodeposition rates and sediment erosion) for an intertidal mudflat in relation to changes in current velocity and benthic macrofauna. In: Black KS, Paterson DM, Cramp A (eds) Sedimentary processes in the intertidal zone. Special Publication No. 139. The Geological Society, London, p 85–97

Williamson TR, Tilley DR, Campbell E (2015) Emergy analysis to evaluate the sustainability of two oyster aquaculture systems in the Chesapeake Bay. Ecol Eng 85: 103–120

Wilson PS, Vopel K (2015) Assessing the sulfide footprint of mussel farms with sediment profile imagery: a New Zealand trial. PLOS ONE 10:e0129894

Wootton JT (2002) Indirect effects in complex ecosystems: recent progress and future challenges. J Sea Res 48: 157–172

Xia XH, Yang ZF, Huang GH, Zhang XQ, Yu H, Rong X (2004) Nitrification in natural waters with high suspended-solid content — a study for the Yellow River. Chemosphere 57:1017–1029

Xia X, Yang Z, Zhang X (2009) Effect of suspended sediment concentration on nitrification in river water: importance of suspended sediment–water interface. Environ Sci Technol 43:3681–3687

Xia X, Liu T, Yang Z, Michalski G, Liu S, Jia Z, Zhang S (2017a) Enhanced nitrogen loss from rivers through coupled nitrification–denitrification caused by suspended sediment. Sci Total Environ 579:47–59

Xia X, Jia Z, Liu T, Zhang S, Zhang L (2017b) Coupled nitrification–denitrification caused by suspended sediment (SPS) in rivers: importance of SPS size and composition. Environ Sci Technol 51:212–221

Yao X, Zhang L, Zhang Y, Xu H, Jiang X (2016) Denitrification occurring on suspended sediment in a large, shallow, subtropical lake (Poyang Lake, China). Environ Pollut 219:501–511

Yu Z, Zhong X, Yu C, Wang C, Duan P, Wen L, You Y (2017) Characteristics of nutrient release from sediments under different flow conditions. Chem Spec Bioavail 29:70–77

Zhu W, Wang C, Hill J, He Y, Tao B, Mao Z, Wu W (2018) A missing link in the estuarine nitrogen cycle?: Coupled nitrification–denitrification mediated by suspended particulate matter. Sci Rep 8:2282

Ziebis W, Huettel M, Forster S (1996) Impact of biogenic sediment topography on oxygen fluxes in permeable seabeds. Mar Ecol Prog Ser 140:227–237